STATISTICAL MODELING AND OPTIMIZATION OF MECHANICAL PROPERTIES FOR SOLIDIFIED POLYLACTIC ACID PARTS FABRICATED BY FUSED FILAMENT MODELING PROCESS

A Dissertation submitted

in partial fulfillment of the requirements

for the degree of

MASTER OF ENGINEERING

in

PRODUCTION ENGINEERING

by

JAGDISH KHATWANI

801482012

Under the Supervision of

DR. VINEET SRIVASTAVA

MECHANICAL ENGINEERING DEPARTMENT

THAPAR UNIVERSITY, PATIALA

JUNE, 2016

CERTIFICATE

I hereby declare that the thesis entitled, **"STATISTICAL MODELING AND OPTIMIZATION OF MECHANICAL PROPERTIES FOR SOLIDIFIED POLYLACTIC ACID PARTS FABRICATED BY FUSED FILAMENT MODELING PROCESS"**, is an authentic record of my study carried out as requirement for the award of degree of **MASTER OF ENGINEERING (PRODUCTION ENGINEERING)** at **THAPAR UNIVERSITY, PATIALA** under the guidance of **DR. VINEET SRIVASTAVA, Assistant Professor, Mechanical Engineering Department, Thapar University, Patiala** during **July 2014 to June 2016**. The matter embodied in this report has not been reported in part or full to any other university or institute for the award of any other degree.

Date: 14/07/2016

Khatwani J.H.

Jagdish Khatwani
Reg. No. 801482012

This is to certify that above declaration made by the student is correct to the best of my knowledge and belief.

14/07/2016

DR. VINEET SRIVASTAVA
Assistant Professor
Mechanical Engineering Department
Thapar University, Patiala- 147004

Countersigned by

Dr. S.K. Mohapatra
Head, Mechanical Engineering Department
Thapar University, Patiala-147004

Dr. S.S Bhatia
Dean of Academic Affair
Thapar University, Patiala-147004

Acknowledgement

I would like to thank all the people who contributed in some way to the work described in this thesis. First and foremost, I thank my thesis supervisor **Dr. Vineet Srivastava, Assistant Professor, Mechanical Engineering Department, Thapar University, Patiala** for his guidance, support, inspiring suggestions and for the development of thesis at every step. He took keen interest in my report and helped me to access facilities of Mechanical Engineering Department laboratories.

I would also like to acknowledge with much appreciation the role of **Dr. P.M Pandey, Associate Professor, IIT Delhi** for giving me the permission to use the Rapid Prototyping Lab at IIT Delhi as and when required. I am also thankful to MED faculty at Thapar University, Patiala for their support and encouragement.

I would also like to thank **Dr. S.K. Mohapatra, Head & Senior Professor, Mechanical Engineering Department, Thapar University, Patiala** for providing facilities for completion of the work.

A special thanks to my friends Shekhar Saini, Pankaj Singla, PhD scholar Mr. Amrinder Singh (Thapar University) and Mr. Varun Sharma (IIT Delhi) for their help and support during thesis work.

In the end, I wish to express my deep sense of gratitude to my family, for supporting and encouraging me at every step of my work. It is the power of their blessings, which has given me the courage, confidence and zeal for hard work.

Khatwani J.H.

Jagdish Khatwani

ABSTRACT

3D Printing is a layered manufacturing process that builds prototypes by depositing material in layered form using heaters. Prototypes made by 3D Printing are widely used in product development as they can be used for product testing. Prototypes should have a very good mechanical properties for functional performance as well as aesthetics. The mechanical properties in 3D printing depends upon different process parameters, namely Layer Thickness, Nozzle Diameter, Part Bed Temperature, Speed of Deposition, Raster Angle of Deposition, Raster Width and Length of the parts. In this present work, an attempt has been made to improve the mechanical properties namely, tensile strength, flexural strength and impact strength of prototypes of Solidified PolyLactic acid parts fabricated using Fused Filament Modelling process of 3D Printing. Experiments have been performed according to Central Composite Rotatable Design (CCRD) considering three parameters namely layer thickness, nozzle diameter and part bed temperature of parts at three levels. Empirical statistical models have been developed for predicting the tensile strength, flexural strength and impact strength of the parts. Analysis of variance (ANOVA) has been used to test the significance of process variables on these mechanical properties. In case of tensile strength, layer thickness and part bed temperature are found significant parameters. Flexural strength is mainly affected by layer thickness, followed by part bed temperature and nozzle diameter. In case of impact strength, layer thickness and nozzle diameter are found to be significant. Confirmation of statistical model have been done by estimating the error and performing experiments at different parameters other than experiments in DOE and the results were found to be satisfactory. Optimization for the maximization of tensile strength, flexural strength and impact strength have been done using trust region based MATLAB technique. SEM has been used to understand the mechanics of fracture in testing for tensile strength, flexural strength and impact strength.

Keywords: 3D Printing, PolyLactic Acid, Tensile Strength, Flexural strength, Impact strength, Part Bed Temperature, Layer Thickness, Nozzle Diameter

CONTENTS

LIST OF FIGURES

LIST OF TABLES

NOMENCLATURE

3D	3 Dimensional
ABS	Acrylonitrile Butadiene Styrene
ANOVA	Analysis of Variance
ASTM	American Society for Testing and Materials
CAD	Computer Aided Design
CAE	Computer Aided Engineering
CAM	Computer Aided Manufacturing
CCRD	Central Composite Rotatable Design
DF	Degree of Freedom
FDM	Fused Deposition Modelling
FFM	Fused Filament Modelling
FS	Flexural Strength
HIPS	High Impact Polystyrene
IS	Impact Strength
ISO	International Organization for Standardization
LOM	Laminated Object Manufacturing
LENS	Laser Engineered Net Shaping
MS	Mean of Square
ND:YAG	Neodymium-Doped Yttrium Aluminium Garnet
PC	Polycarbonate
PET	Polyethylene Terephthalate
PLA	PolyLactic Acid
RP	Rapid Prototyping
RSM	Response Surface Methodology
SL	Stereolithography process
SEM	Scanning Electron Microscope
SLS	Selective Laser Sintering
STL	STereoLithography file format
SS	Sum of Square
TS	Tensile strength
βi βii βij	Beta (constant Coefficient)
Y	Response
N	Total number of experiments
α	Level of confidence interval
ε	Random error

CHAPTER 1
INTRODUCTION

1.1 RAPID PROTOTYPING

The development of the product in very short amount of time in the competitive market is a huge problem. For a firm to become successful in market, they have to gain edge over the competitors by reducing product development time. In order to achieve this there are many factors which play critical role like introduction of new materials, changing technology to reduce designing and manufacturing time and rapidly changing customers need. This results in the development of new process known as Rapid prototyping (RP).

RP technology is closely tied with development of application of computers in the industry. However, examining the numerous RP systems in existence today, it can be deduced that many technologies and advancements like computer aided design, manufacturing systems and materials have been crucial in the development of RP systems. Prototyping began as early as humans started to developed tools. The techniques used to making these prototyping tended to be craft based and labour intensive. This phase was defined as the first phase of prototyping also called as manual prototyping. In early 1980's as the application of CAD/CAM/CAE gathered wide spread approval, the second phase of prototyping called virtual prototyping evolved. The computer generated models could now be tested, analyzed and modify in a similarly way as the physical prototype. However, these tools also helped in making the products and there prototypes even more complex requiring more time for physical realization. This necessitated the advent of solid freeform fabrication or layered manufacturing or rapid prototyping of physical parts, which represented the third phase in the evolution of prototyping. The invention of RP methodologies became important because of exceptional time saving for complicated models and difficult to produce parts, which was not present earlier.

"A Prototype is the first or the original example of something that has been or will be copied or developed; it is a model or a preliminary version. It can also be defined as an approximation of a product or system or its components in some form for a definite purpose in its implementation." **[1]**

1.2 BASIC PRINCIPLE OF RAPID PROTOTYPING PROCESS

RP process is an additive production process in which there is no material removal. RP process makes the model by accumulating layers in required shape on an x-y plane. The z axis is generated by stacking one layer over the other, thereby realizing the product. The method of fabrication of RP parts is shown in figure 1.1 and steps followed by all commercial RP processes are given below:

1. A 3D CAD model is designed in design software and file is renewed in to STereoLithography (STL) file format by tessellating the geometry.
2. STL file is checked for errors like gaps, self intersecting facets, dangling edges, flip triangles etc. and if defects are detected, the files are repaired.
3. The orientation of the specimens is checked and defined as per requirement of the product.
4. Various slicing software are used to generate data of sliced layer of the model for RP systems by using STL file as an input. Here to control the parameters like slice thickness is defined because they are important factor for building time and surface quality.
5. First layer of model is created by using different deposition principle of different RP machines. The podium is lowered equal to one slice thickness and the task is repeated until the model is complete.
6. Final step is post processing where supports are separated. Than face of model is cleaned and finish.

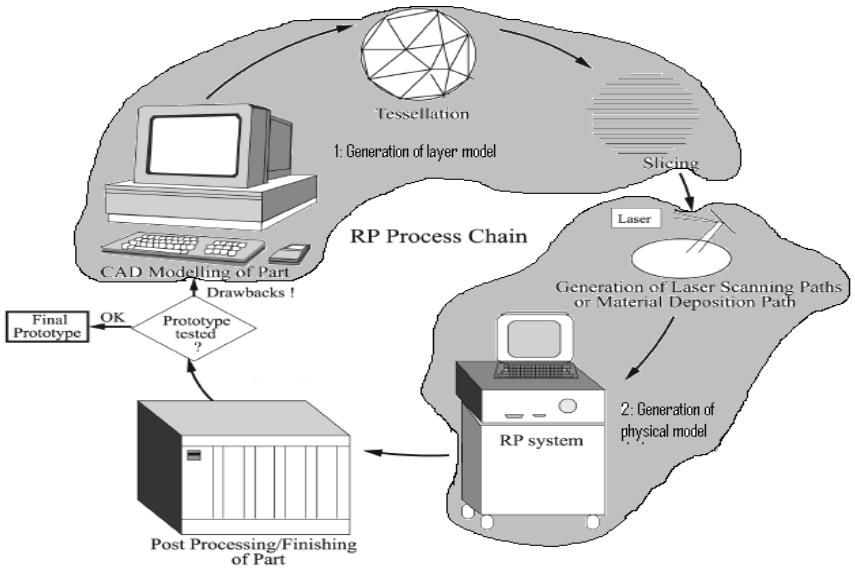

Figure 1.1 RP Process Chain [2]

Rapid prototyping processes can be divided into different groups according to their layer formation of materials to build the physical model. Various RP systems such as Stereolithography, Fused Deposition Modeling, Laser Engineered Net Shaping, Selective Laser Sintering, Laminated Object Manufacturing, and 3D Printing are commercially available today.

Stereolithography (SL) process is shown in figure 1.2. This technique was patented in 1986 and changed the history of rapid prototyping. Here, solid polymers are formed by photosensitive liquid resin when exposed to ultra violet light. In this process laser traced the first layer and raised area is lowered as per layer thickness and left for petite time to facilitate liquid polymer settle to a smooth and level surfaces and reduce fizz formation. The main cause of bonding of one layer over other layer is self adhesive property of the materials [A].

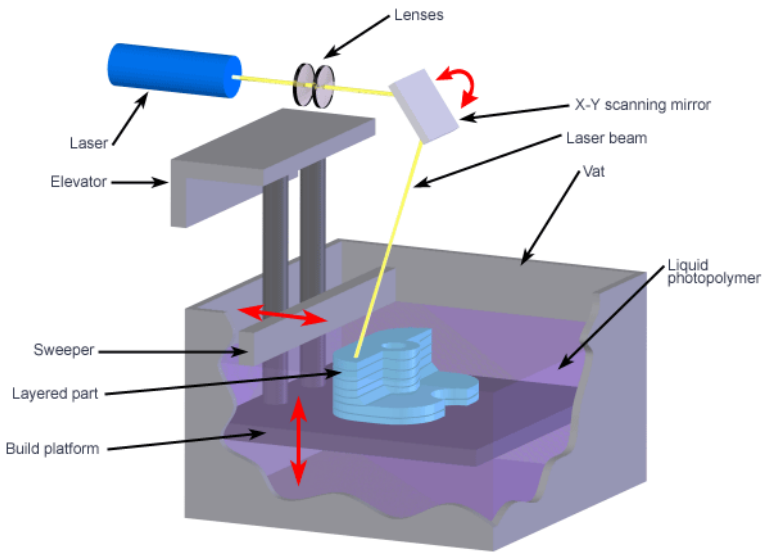

Figure 1.2 Schematic View of Stereolithography Process [B]

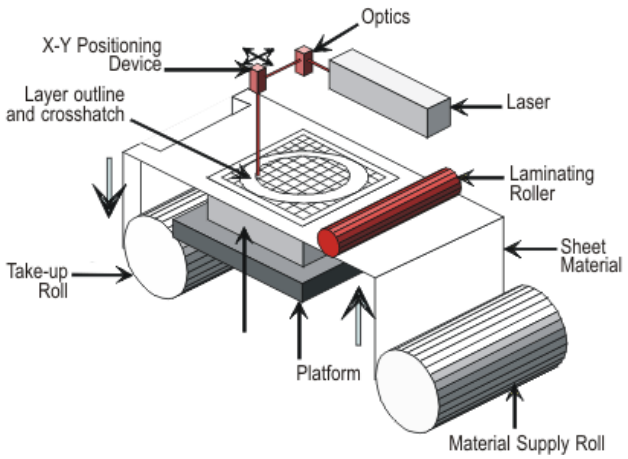

Figure 1.3 Laminated Object Manufacturing Process [C]

The schemetic of **Laminated Object manufacturing (LOM)** process used the materials like plastic, metal laminates and adhesive coated paper, is shown in figure 1.3. In this process hot roller is used for bonding of layers, which activates a heat sensitive adhesive which makes bond between layers. The traced of each layer is cut with a laser which is penetrating up to layer thickness. It is used where large and high volume prototypes are required [2].

Selective laser sintering (SLS) process included the melting and subsequent solidification of the part material which is in powder form. In this process, before starting of sintering, curling is minimized to avoid bending by raising the bed temperature to its melting temperature by infrared heating. After it, laser scans the layer of powder and increases the temperature to near the melting where fusion of the powder occurs to form solid parts. Last step is lowering the bed by one layer thickness and powder is swelling for another layer by rotating roller. The cycle is repeated until the part is completed [3]. Figure 1.4 shows the steps of layer by layer manufacturing in SLS process.

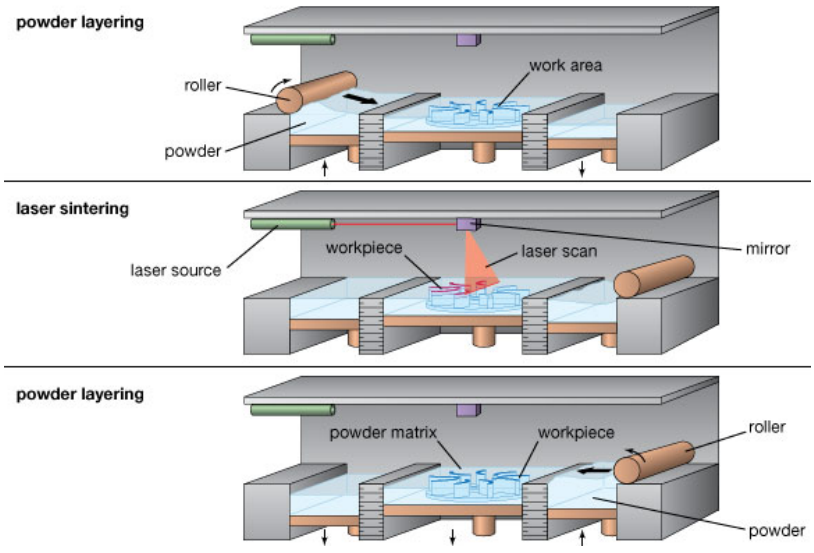

Figure 1.4 Selective Laser Sintering Process [2]

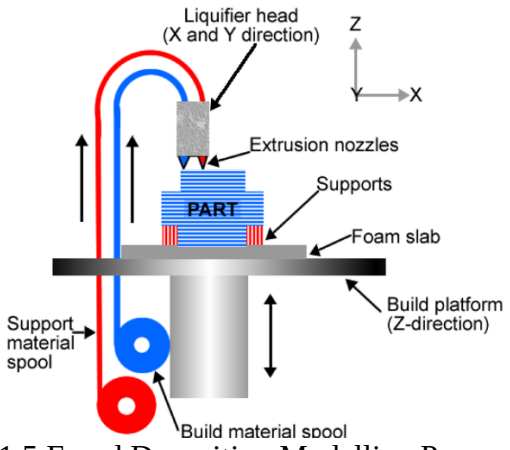

Figure 1.5 Fused Deposition Modelling Process [D]

Fused Deposition Modeling (FDM) process uses a nozzle which is conveyable in x-y directions and extrudes the molten plastic materials. Figure 1.5 shows schmetic of FDM process. The temperature of fabricate material is faintly greater than its melting temperature due to which it solidifies in short interval of time and joined to preceding layer by cold welding. At present, FDM process used different nozzles for part material and support material. The support material can be easily removed due to its poor quality as compare to part material [2].

Three-dimensional Printing (3D Printing) uses ink jet technology to build the parts. The machine spread the layers of materials in the powder form which are bonded by adhesive from ink jet printer head. Some machines based on photo polymerisation used ultra violet laser situated in the print head to deposit each layer. In this process we don't require any support because powder bed itself support overhangs. In wire based 3D printing technique, dispensable material in the form of wire is fed and the heater raises the temperature to generate a continuous semi melt droplet of the material. The head moves in x-y plane to generate a layer. Figure 1.6 explains 3D printing technique.

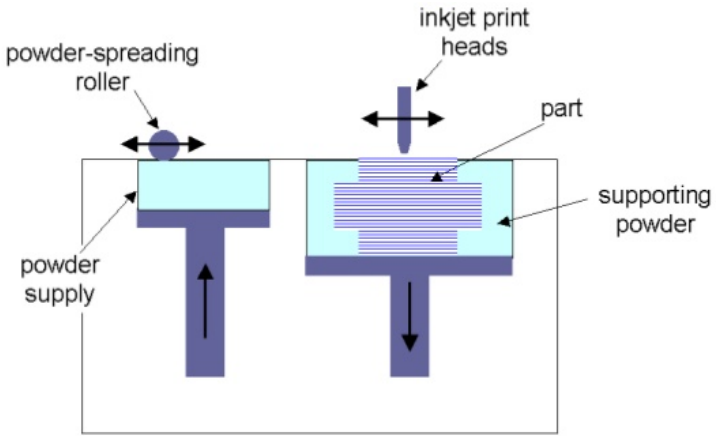

Figure 1.6 3D Printing Process [E]

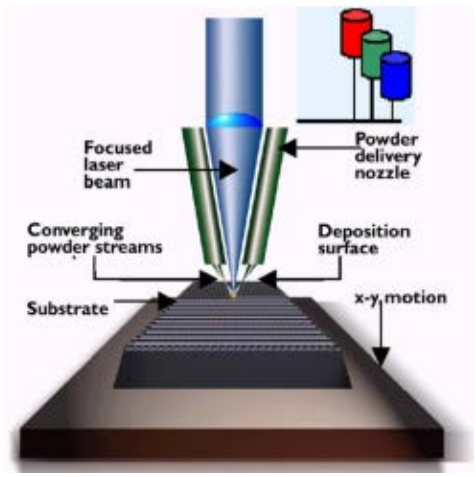

Figure 1.7 Laser Engineered Net Shaping Process [C]

Laser Engineered Net Shaping (LENS) process, as shown in figure 1.7, creates a molten puddle on the surface by comprised a high power ND: YAG laser. Here, laser marks the cross section of the part being created by using a "printing" motion system which moves the platform horizontally. When formation of layer was finished, the machine's powder delivery nozzle moves up for setting up next layer. Typically the prototypes could need extra finishing however, they're absolutely dense product with excellent grain formation [2].

There are other types of RP processes also available. The classification of rapid prototyping is given below in fig 1.8.

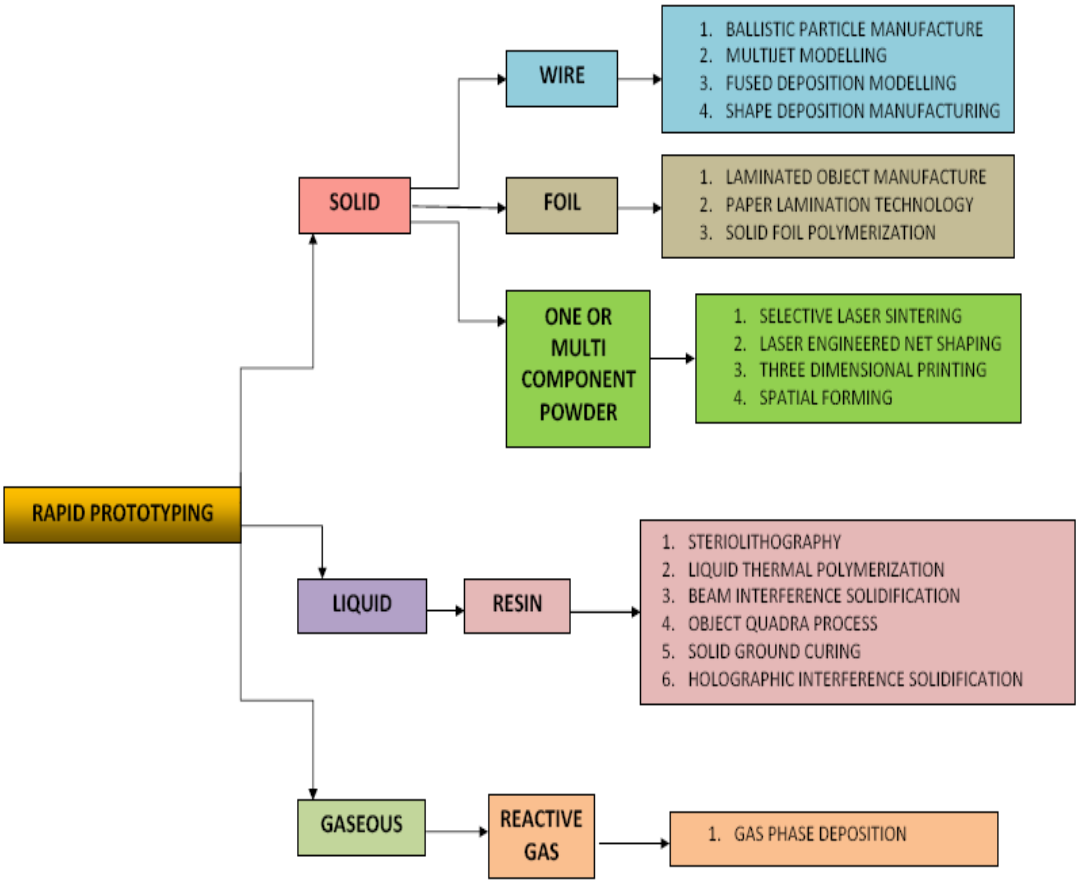

Figure 1.8 Classification of RP

1.3 PROBLEM AREA OF RP

Even as RP is an efficient and fast method for producing parts with different materials but it has not attained prevalence because of the inferior mechanical properties of raw material used. Following are some of the problem area of the RP:

1. **Strength** of the RP parts is low as compare to part fabricated by conventional machining.

2. **Dimensional Accuracy** is compromised due to shrinkage of material.
3. **Surface Roughness** of the part is high due to stair-stepping effect and removal of support material from outer surface.
4. **Build time** is depends directly on surface finish, if we want high surface finish time required to build would be high.
5. **Support structure** is desirable structure; its function is to support the overhanging part. Removal of support structure from part fabricated may cause surface damage and affect the surface finish.
6. **Shape factor** is the volumetric distortion of the part due to uneven shrinkage.

1.4 FUSED FILAMAENT MODELLING (FFM)

1.4.1 PROCESS

Fused Filament Modelling is a process in which a machine drops a constant supply of molten filament (like a wire) of a certain material (polymers, wax or thermoplastics) to form layers on a platform. Successive layers are joined by heat and/or adhesion.

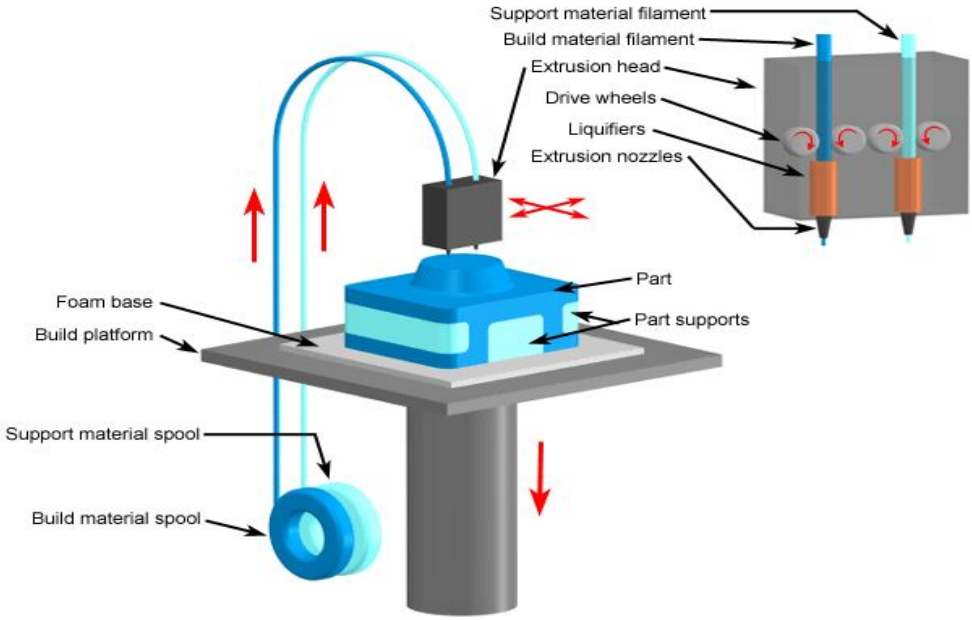

Figure 1.9 Schematic View of FFM [F]

In FFM process, thermoplastic string is fed in to a heated nozzle whose temperature is greater than the glass transition temperature of the material by which material are extruded through nozzle. It moves in XY gentry as per path defined by slicing software and print one layer of part. Once the layer is on bed, the part bed moves down by the distance of one layer thickness so that the next one can be printed. The

process goes on one layer over other until the part is fabricated. The layer thickness identifies number of layers in a part. In this process, material flow through nozzle which is translated over pre-defined path on a build platform. The extruded material solidifies within a short span of time. Figure 1.9 represents the schematic view of the process. Thermoplastic material is passed through heated nozzle on to build platform. The nozzle head moves in XY direction where as build platform moves in the Z direction. The movement of nozzle and build platform is controlled by numerical controlled method.

The major advantages of the FFM process are printing of durable parts with variety of materials and its small size due to which it can used in office environment. In recent times, most FFM systems used two extrusion nozzles –first for the structural build material and second for the removable support material. Once the fabrications of the parts are completed, it is carefully removed from the build plate.

1.4.2 PROCESS PARAMETER OF FFM

Since FFM is an extrusion kind method, the high-end FFM machines supply variety of method parameters, which put aside the client to manage the form, dimension, and internal structure of the half to be created. This enables the user to fabricate parts ranging from fully solid to a honeycomb structure with varying part strength, surface quality, accuracy, and mechanical properties. These characteristics also affect the build time.

The main parameters which can be user specified are slice height (layer thickness), model tip diameter, build orientation, model build temperature, part fill style, part interior style, raster width, raster angle, and raster air gap. A user is required to select these parameters when pre processing the STL file on the FDM software. Some of these parameters are defined below.

Layer Thickness: Slice height is the layer thickness at which the STL model is sliced for part building. The distance traveled by bed to build consecutive layers in z-direction called layer thickness. Build time and surface finish of surfaces are directly proportional to layer thickness. The value of selected slice height depends upon the type of FFM process, model tip size, and type of FFM material used. The model tip size used on the FFM machine allows a specified layer thickness value.

Model tip size: Model tip size is the diameter of the model material extrusion nozzle. The tip is screwed at the bottom of the print head. FFM systems provide a set of tips. Each tip size allows a range of layer thickness and road width to be used.

Model build temperature: Model build temperature is the temperature of the heating ingredient for the part fabrication in the print head. It pedals the flow of molten material which is comes out from the tip.

Raster width: Raster width or road width is the width of the bead deposited from the model tip on a layer.

Build Orientation: It is the position of the part on the bed at which it is manufactured.

Extrusion speed: It is distance covered by the nozzle in one second during deposition of material.

1.4.3 MATERIALS USED IN FFM PROCESS

In 3D printing variety of materials, such as ABS and PLA plastics, glass filled polyamide, stereolithography materials (epoxy resins), polyamide (nylon), silver, titanium, steel, wax, photopolymers and polycarbonate. Acrylonitrile Butadiene Styrene **(**ABS**)** and Polylactic acid (PLA) are most popular printing materials. High Density Polyethylene (HDPE) plastic is used when higher density of the part is required. Sometimes ABS HDPE blend is used to improve mechanical properties. Some of the low melting point metals can be printed but it is not popular.

1.5 MOTIVATION

It has been observed that properties of RP parts are influenced by different processing parameters. Proper adjustment of these process parameters can improve the various properties of RP parts. RP parts are also used as pattern in sand casting, vacuum casting and investment casting. In actual conditions, to resist various type of loading, parts must have good mechanical properties. Mechanical properties become critically important where the stiffness, surface finish and strength are required to meet in-service loading requirements. It is necessary to study the effect of various process parameters on mechanical properties because mechanical properties influence the behaviour of functional parts.

1.6 THESIS ORGANIZATION

The thesis is described in SEVEN chapters.

Chapter 1 comes out with an introduction to RP processes. An overview of FFM process and its potential applications are presented. The motivation for present research attempt is discussed followed by organization of this thesis.

Chapter 2 describes current state of the art and research literature in the proposed area of research. Major contributions made in the past covering the reaserch on mechanical properties of different materials in various RP processes have been covered. The chapter also justifies the need for undertaking present research work.

Chapter 3 discusses the response surface methodology for experimentation. It also discusses the implementation procedure with selection of process parameters.

Chapter 4 describes the statistical modelling of tensile strength. The significant process parameters have been identified and the details of response surfaces is provided. The details of accuracy and optimization of model have been given.

Chapter 5 describes the experimental studies for flexural strength. Statistical models of flexural strength has been developed. The significant process parameters have been identified and the details of response surfaces is provided. The details of accuracy and optimization of model have been given.

Chapter 6 describes the statistical modelling of impact strength. The significant process parameters have been identified and the details of response surfaces is provided. The details of accuracy and optimization of model have been given.

Chapter 7 summarizes the major findings (conclusions) of the present research work and directions for future research have been highlighted.

CHAPTER 2
LITERATURE REVIEW

2.1 INTRODUCTION

The basic procedure in different RP technique is layer by layer manufacturing, but all RP processes have different input variables that affect the feature of the product corresponding to the surface roughness, strength, dimensional accuracy. The basic parameters considered for FFM based 3D printing process are layer thickness, build orientation, part bed temperature, nozzle diameter, raster width, hatch spacing etc. many work is done on surface roughness of RP systems to overcome it by applying different approaches based on their process parameter. Here a brief study has been done on the different parameter affecting the mechanical properties of RP systems.

2.2 LITERATURE REVIEW

There are several attempts made to develop a model for mechanical properties of RP parts fabricated by different processes.

Ahn et al. (2006) [4] investigate the properties of ABS parts fabricated by the FDM. Using a Design of Experiment (DOE) approach, the process parameters of FDM, such as raster orientation, air gap, bead width, colour, and model temperature were examined. It is concluded from the experimentation that air gap and raster orientation affects the tensile strength greatly. Tensile strengths and compressive strengths of directionally fabricated specimens were measured and compared with injection moulded FDM ABS P400 material. For the FDM parts made with a 0.003 inch overlap between roads, the typical tensile strength ranged between 65 and 72 percent of the strength of injection molded ABS P400.

Ang et al. (2006) [5] investigated the effect of porosity on the mechanical properties in fused deposition modelling (FDM) fabricated parts. Porosity and mechanical properties of acrylonitrile butadienene-styrene (ABS) scaffold structures were investigated by considering parameters namely, air gap, raster width, build orientation, build layer and build profile, on in two designed experiments. From the statistical analysis, it was found that air gap had the largest effect on the compressive strength of the scaffolds. An increase in air gap result in decrease in compressive strength. Whereas increase in raster width, increased the compressive strength of the porous structure.

Jain et al. (2008) [6] show how the parts strength and delay time is interrelated in SLS process. They fabricate parts for different ranges of delay time using the polyamide powder. All experiments were repeated thrice for repeatability for seven different delay time ranges, ranging from 0–0.049 s in the increments of 0.007 s. Parameters taken in consideration were layer thickness (0.15 mm), hatch spacing (0.3 mm), scan speed (4,500 mm/s). Optimum delay range found was 0.014-0.021 s.

Bagisk et al. (2010) [7] studied the influence of the orientation and the structure of the manufactured parts by FDM. Material used was Polyetherimide (PEI). Sample parts for tensile and compression testing were generated. Tensile specimen were generated in three different direction X,Y and Z, compression specimen were fabricated in XY and Z direction, which is shown in figure 2.1.

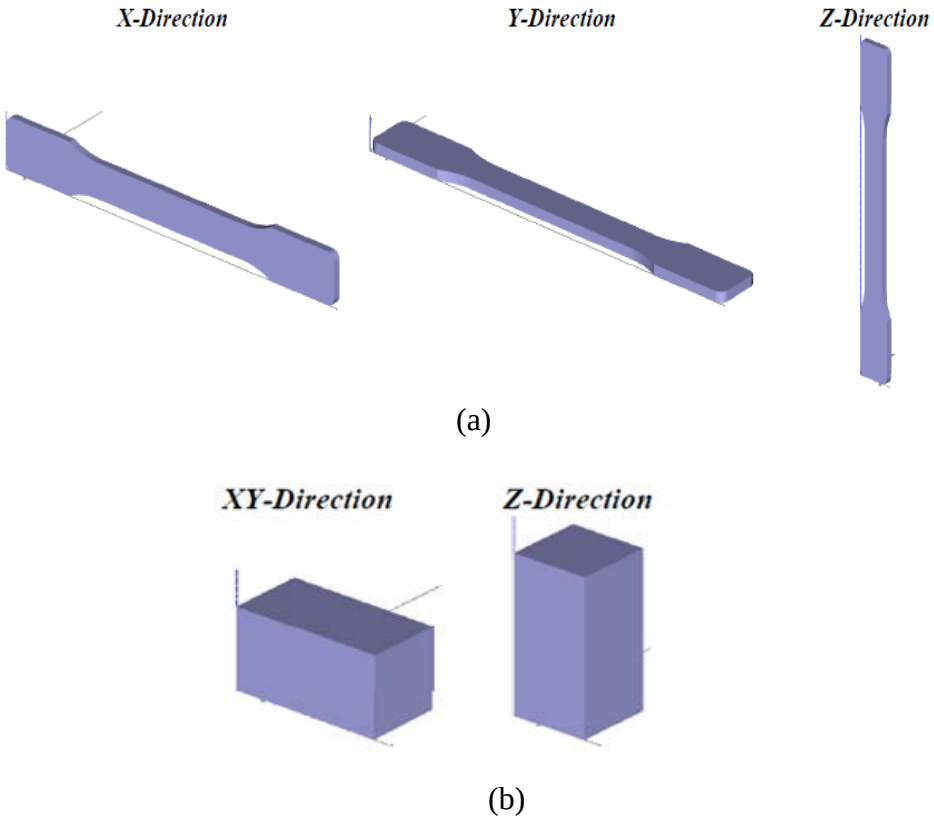

Figure 2.1 Part build orientation for (a) Tensile specimen, (b) compression specimen [7]

The test result showed that tensile specimen build in X direction has highest tensile strength (63 Mpa), specimen build in Y direction has lower (45 Mpa) and in Z direction lowest strength (40 Mpa).Compressive strength of part build in XY direction is lower (82 Mpa) than Z direction (96 Mpa).

Kesy et al. (2010) [8] proved that the orientation of the produced parts in the polymer jetting technology machine is the main factor which influences their mechanical properties. As shown in figuur 2.2, tensile parts were fabricated in three different direction say XY, YZ and ZX. The test bars produced in the YZ orientation have the highest mechanical properties whilst these produced in the ZX orientation have the smallest mechanical properties. The difference of tensile strength between 2nd and 1st was 3.6% and the difference between 2nd and 3rd orientation was 29%, while the difference of elongation at break between 2nd and 1st was 60.4% and difference between 2nd and 3rd orientation was 65.6%.

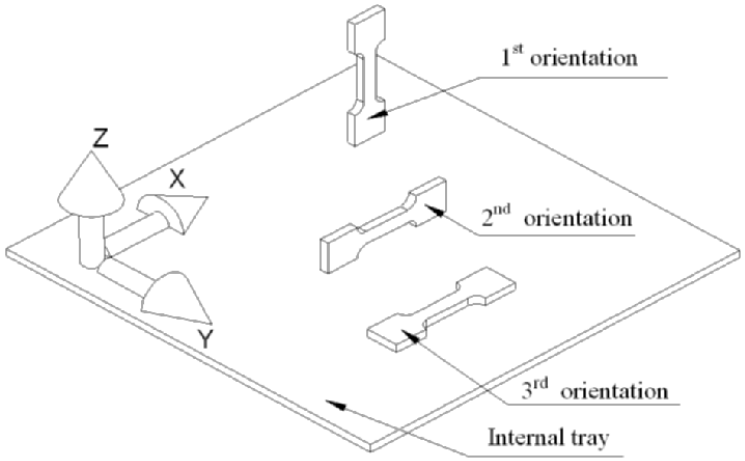

Figure 2.2 Part build orientation [8]

Percoco et al. (2012) [9] concluded that compressive strength can be improved when the it is treated with chemical solution. Results shoed that compressive strength is increased by 2 to 4 percent , when FDM prototypes treated with a solution of 90% dimethylketone and 10% water with raster angel and raster width is taken as process parameters. There is increase in tensile ductility but also to slightly lower tensile strength and 3 point bending test showed general improvement in flexuralstrength.

Croccolo et al. (2013) [10]investigated the mechanical behavior of the Fused Deposition modelled parts using ABS material, once the raster pattern (dimensions, number 20 of contours, raster angle) has been stated. They conclude that that greater the contour line greater the stiffness and strength but increase in brittleness of material. The effectiveness of the theoretical model has been verified by comparison to a significant number of experimental results, with mean errors of about 4%.

Afrose et al. (2015) [11] investigated the fatigue properties of PLA parts produced by FDM process. ASTM D638 standard was followed for testing. Experimental testing was cyclically performed at 80, 70, 60 and 50 % nominal values of the ultimate tensile stress. Results showed that tensile strength is higher for parts in X build orientation as compared to those built in Y and 45 degree orientations. But fatigue life is higher for the part built in 45 degree orientation as compared to the parts build in X and Y orientation.

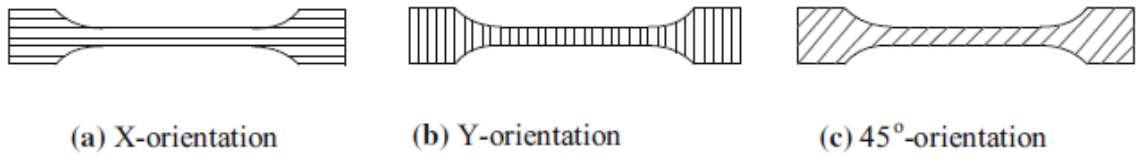

Figure 2.3 Deposited toolpath pattern in three build orientations [11]

Roberson at el. (2015) [12] investigated the effect of stress concentrator fabrication on 3D printed parts using ABS, PC, PC-ABS, and Ultem 9085 as material. Izod impact testing showed that samples printed on the XY plane at 45◦were shown to have the greatest resistance to impact and samples printed vertically in the ZXY orientation had the lowest resistance to impact. Only samples printed from Ultem 9085 experienced a significant difference in impact strength when comparing stress concentrator fabrication method of specimens by printing and milling to develop stress concentrator.

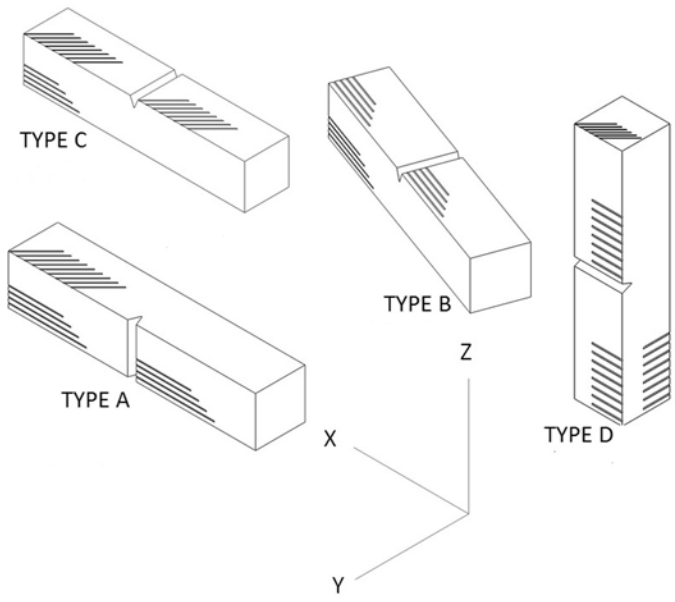

Figure 2.4 The different build orientations and notch placements [12]

Table 2.1 presents a summary of the major studies conducted for different mechanical properties in different rapid prototyping process.

Table 2.1 Major Research Effort for mechanical properties in RP Process

Investigators	Machine/ Process	Process Parameters	Responses
Ang et al.. (2006)	FDM	Air gap, Raster width, Build orientation, build lay down pattern, build layer	Air gap and raster width affects the compressive modulas most.
Ahn et al. (2006)	FDM	Air gap, Road width, Model temperature, colour, orientation	Negative air gap improves the tensile strength of part.
Pandey et al. (2008)	SLS	layer thickness, hatch spacing, scan speed	Optimum delay time will result in improved strength
Bagisk et al. (2010)	FDM	Part build orientation	Higher tensile strength when X orientation, higher compressive strength when Z orientation
Kesy et al. (2010)	Polymer jetting technology (3D printing)	Part build orientation	Highest strength in XY direction lowest in ZX direction.
Croccolo et al. (2013)	FDM	Build orientation, number of contour lines, bead width, raster angle, air gap, layer thickness	Greater contour will increase stiffness and strength but it will increase the brittle behavior of the part.
Afrose et al. (2015)	FDM	Orientation	Part build in X direction shows higher tensile strength, and at 45◦ to X and Y direction shows highest fatigue strength.

2.3 RESEARCH GAP

From literature survey, it has been observed that maximum work regarding part strength is concerned on FDM, SLS and 3D printing technologies. It has also been observed that very few work is done in strength analysis of parts fabricated through Solidified PLA as compared to the ABS. In 3D printing, one of the most widely used

material is PolyLactic Acid (PLA), which has gained wide popularity because of its high strength, durability, light weightness, ready availability and a lesser tendency to wrap.

2.4 RESEARCH OBJECTIVE

The objectives of this project work are:

1. To develop the statistical models for mechanical properties, such as tensile, flexural, impact strength of PLA parts using 3D printer based on FFM process.
2. To study the effect of process parameters on tensile, flexural, impact strength.
3. To estimate the error in the developed models.
4. To validate the developed tensile, flexural and impact models.
5. To obtain the optimum process parameters for maximum tensile, flexural and impact strength of the parts.

2.5 PLANNED METHODLOGY

The present work aims on finding out the effect of process parameters namely part bed temperature, nozzle diameter and layer thickness on mechanical properties. To solve this problem steps are follow as :

1. Selection of process variables and their levels according to machine specifications.
2. Solid modelling of standard test specimens according to established standards.
3. Construction of Design of experiments (DOE) using CCRD method of response surface technique.
4. Fabrication of parts according to DOE.
5. Experimental testing of the fabricated parts according to standards (ASTM,ISO).
6. Analysis of Variance for analyzing main effect and to find out significant parameters.
7. Developing of statistical model for tensile, flexural and impact strengths.
8. Estimation of error for developed models.
9. Optimization of process parameters by using trust region based optimization method using MATLAB.
10. Validation of the models by comparing experimental and theoretical measurement of the above developed models.

CHAPTER 3

STASTICAL MODELING USING CENTRAL COMPOSITE ROTATABLE DESIGN

3.1 RESPONSE SURFACE METHODOLOGY

In single variable experiment planning, a huge number of experiments have to be performed as we increase the process variables and their levels. For developing the equation of response surfaces, there are many experimental designs which uses small no of experiments to proximate it. There are two models which are used in RSM. The primary is first degree model (d=1),

$$y = \beta_0 + \sum_{i=1}^{n} \beta_i x_i + \varepsilon \quad (1)$$

And the second degree model (d=2)

$$y = \beta_0 + \sum_{i=1}^{k} \beta_i x_i + \sum \sum_{i<j} \beta_{ij} x_i x_j + \sum_{i=1}^{k} \beta_{ii} x_{ii}^2 + \varepsilon \quad (2)$$

Where x= input variables

y= response of interest

β= constant coefficients

ε = random experiment error

The functions of using these models are:

1. To create a correlation between y and input variables which is useful for developing statistical model to predict outputs value for given values of input parameters.
2. To establish the importance of factors on response.
3. To calculate the most favourable setting of input variables that result in (maximum/minimum) answer over a certain range of variables.

First order model is satisfactory where we have a small range of parameters. This model is also not suitable for analyzing maximum, minimum values of responses. Second degree model is used for response surface with parabolic curvature. It describes quadratic surfaces which can easily represent highest, lowest, crease or encumber point. It gives curve plot which is supportive to visualize of surface when variables are greater than three. This representation is flexible due to its variety of functional form. So, the experiments are conducted to obtain second degree model [13].

Fitting of second order quadric model can be done by many designs namely, full factorial design and CCRD. The number of experiments increases exponentially as it depends on 3^N (where N= number of variables) in full factorial design. So it becomes

impractical. CCRD is very efficient design technique for second degree model because it improved by additional centre and axial points to allow approximation of improvement parameters of model. Figure 3.1 shows the CCRD design for 3 variables. It contains 2^N factorial points, 2N axial points and 1 central point. It gives less numbers of experiments as compare to full factorial design [13].

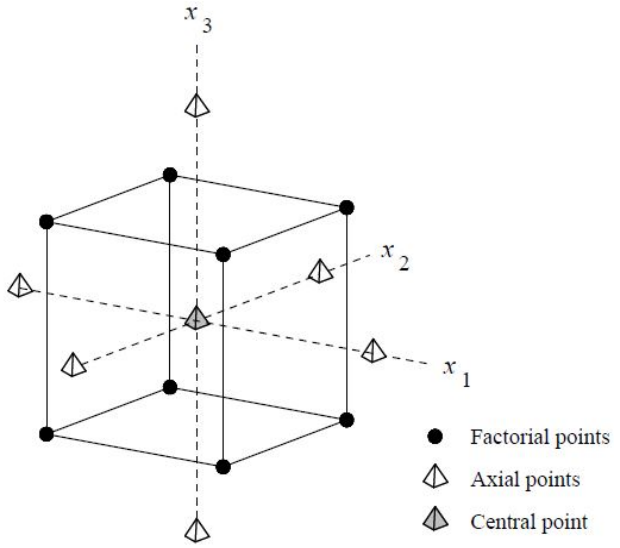

Figure 3.1 Central composite designs for 3 design variables [G]

So as discussed above second order model based on central composite design is best suited for response surface modeling. It quantifies relationship between input process parameters and response surface and as well as give the optimize parameters for best response surface. In this design technique, as given in equation (2), the constant coefficient (β_{ij}) can be found by least square method. In least square method it forms a straight line equation in the form

$$y = \beta x + \varepsilon \qquad (3)$$

here Y is *n* x 1 vector of the observation or called responses, X is an *n* x *s* matrix of the levels of the input variables, β is a *s* x 1 vector of constant coefficients and ε is an *n* x 1 vector of random errors. Thus the least square estimator of β is $b = (X^T X)^{-1} X^T y$. So β vector gives the constant coefficient of the regression model [G].

3.2 PLANNING OF EXPERIMENTS

In present work, our aim is to find the effect of parameters on mechanical properties of the parts. Literature review revealed that among all the factors, parameters such as layer thickness, nozzle diameter and part bed temperature have great influence on mechanical strength of the part. So these parameters are selected for present study. As per

the specification of machine (Protocentre 999 by aha! 3D) given in the machine manual, the range of process parameters are defined. The ranges of layer thickness, part bed temperature and nozzle diameter have been selected as 0.1 to 0.3 mm, 51 to 55^0C, 0.3 to 0.5 mm respectively. Extruder head speed are fixed at 100 mm/sec. The process parameters and their levels are summarized in table 3.1.

Table 3.1: Process Parameters With Their Levels

Parameters	Low Level (-1)	Medium Level (0)	High Level (1)
Nozzle Diameter[ND] (mm)	0.3	0.4	0.5
Layer Thickness[LT] (mm)	0.1	0.2	0.3
Part Bed Temperature[PBT] (degree Celsius)	51	53	55

As PLA materials have many functional properties like high toughness and strength. With PLA, 3D printer is able to fabricate fully functional parts. PLA is used for production tooling and form, fit and function studies. So PLA is selected as build materials. The material, mechanical and thermal properties of PLA is given in the table 3.2-3.4. [H]

Table 3.2 Mechanical Properties [PLA]

Property	**Value**	**Unit**
Hardness. Rockwell R	110-122	
Tensile strength	61-66	MPa
Flexural yield strength	48-110	MPa
Izod Impact, Notched	2.46-2.94	J/cm
Elongation at break	21-30	%

Table 3.3 Material Properties [PLA]

Property	**Value**	**Unit**
Density	1.25	g/cm^3
Melt Flow	18-23	g/10min

Table 3.4 Thermal Properties [PLA]

Property	**Value**	**Unit**
Glass Transition Temperature	52-62	Centigrade
Heat Deflection temperature	49-52	Centigrade

Table 3.5 shows the design of experiments (DOE) plan constructed using central composite rotatable design (CCRD). Three levels of three process parameters gave 20 runs, when central composite full design is constructed, which is shown in table 3.5. There is six central points in full central composite design which is useful to verify the machine accuracy.

Table 3.5 DOE using Central Composite Rotatable Design (CCRD)

StdOrder	RunOrder	Blocks	Nozzle diameter (mm)	Layer thickness (mm)	Part bed temperature (^{0}C)
7	1	1	0.3	0.3	55
14	2	1	0.4	0.2	55
9	3	1	0.3	0.2	53
19	4	1	0.4	0.2	53
20	5	1	0.4	0.2	53
4	6	1	0.5	0.3	51
3	7	1	0.3	0.3	51
5	8	1	0.3	0.1	55
11	9	1	0.4	0.1	53
10	10	1	0.5	0.2	53
17	11	1	0.4	0.2	53
12	12	1	0.4	0.3	53
1	13	1	0.3	0.1	51
15	14	1	0.4	0.2	53
18	15	1	0.4	0.2	53
6	16	1	0.5	0.1	55
8	17	1	0.5	0.3	55
2	18	1	0.5	0.1	51
13	19	1	0.4	0.2	51
16	20	1	0.4	0.2	53

3.3 CAD MODELING AND FABRICATION OF PARTS

The dimensions of the standard test specimens to be modelled according to established standards are shown in figure 3.2.

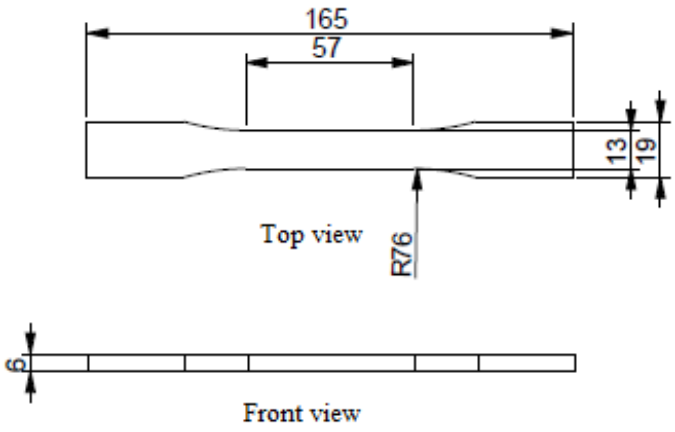

(a) Tensile specimen according to ASTM D 638

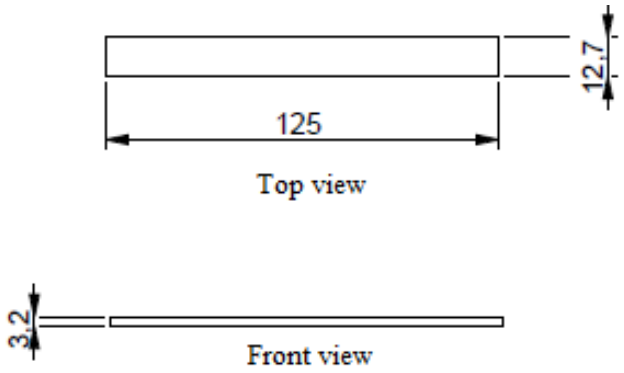

(b) Flexural specimen according to ASTM D790

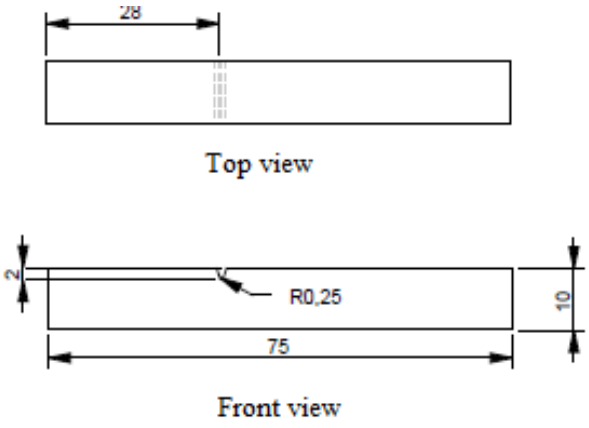

(c) Impact specimen according to IS0 180

Figure 3.2 Dimensions of standard test specimens

On the basis of DOE plan 20 samples for each Specimens are fabricated. The CAD model is designed in creo 5.0 software and converted to STL file format. These STL files were checked in MAGIC software to remove the errors if present any. After this orientation of the parts is set in MakerBoat software. When orientation of the part is set the G codes of the parts are prepared using KISSlicer software. These G codes are fed to the printing machine through SD card and part fabrication is done by machine. The figure 3.3 shows the Protocentre 999 machine and figure 3.4 shows the printed parts for tensile,flexural and impact testing.

Figure 3.3 Protocentre 999 work station (at IIT Delhi)

(a) (b)

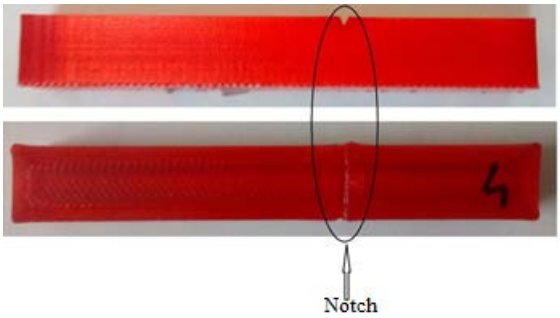

(c)

Figure 3.4 Fabricated specimens of (a) Tensile test (b) Flexural test (c) Impact test

3.4 EXPERIMENTAL TESTING

Figure 3.5 shows the tensile, flexural and impact test performed on different testing instruments. Tensile strength at break is determined on UTE 100 instrument according to ASTM D638 [14] testing standards. Capacity of UTE 100 is 100 KN with minimum resolution of 0.05 KN. Crosshead speed at which testing was done is 5 mm/min. Flexural strength at yield is determined as per ASTM D790-10 [15], in which three point bending test is used for flexural strength determination.

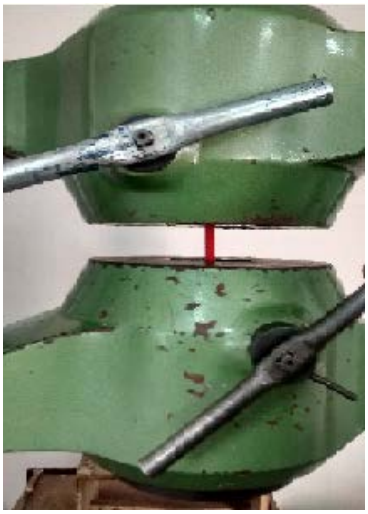

(a)

(b)

(c)

Figure 3.5 Experimentation of (a) Tensile test (b) Flexural test (c) Impact test

The specimen is supported by two supports and loaded in the middle by force until the test specimen fractures. Three point bending test was performed on UTN 20, having capacity of 2000 kgf with minimum resolution of 4 kgf. Crosshead speed was set to 2 mm/min. Izod impact test is performed according to ISO 180 [16]. During impact testing,

specimen is subjected to quick and intense blow by hammer pendulum striking the specimen. The results of tensile, flexural and impact tests are given in the table 3.6.

Table 3.6 Experimental result of Tensile,Flexural and Impact testing

Run-Order	Nozzle Diameter (mm)	Layer Thickness (mm)	Part Bed Temperature (^{0} C)	Tensile Strength (Mpa)	Flexural Strength (Mpa)	Impact Strength (KJ/m^2)
1	0.3	0.3	55	50	76.2	2.677
2	0.4	0.2	55	47	67.2	2.724
3	0.3	0.2	53	43	70.3	2.555
4	0.4	0.2	53	44	65.2	2.496
5	0.4	0.2	53	44	65.1	2.491
6	0.5	0.3	51	34	62.6	2.979
7	0.3	0.3	51	39	71.8	2.752
8	0.3	0.1	55	45	61.4	2.698
9	0.4	0.1	53	47	57.9	2.309
10	0.5	0.2	53	45	66.2	2.679
11	0.4	0.2	53	45	65.0	2.501
12	0.4	0.3	53	41	67.8	2.486
13	0.3	0.1	51	43	60.1	2.648
14	0.4	0.2	53	45	65.2	2.494
15	0.4	0.2	53	44	65.3	2.498
16	0.5	0.1	55	50	62.5	2.676
17	0.5	0.3	55	43	69.6	2.935
18	0.5	0.1	51	50	58.3	2.610
19	0.4	0.2	51	42	62.8	2.736
20	0.4	0.2	53	44	65.1	2.504

CHAPTER 4

STATISTICAL MODELING FOR TENSILE STRENGTH

4.1 STATISTICAL MODELING

A statistical model for the tensile strength was developed, by correlating the input parameters namely nozzle diameter, layer thickness and part bed temperature based on analysis of the data presented in table 3.6, and is given below as equation (4) after eliminating all the insignificant parameters.

$$TS = 19.7 + (195 \times ND) - (504 \times LT) + (0.100 \times PBT) - (300 \times ND \times LT) - (2.50 \times ND \times PBT) + (11.2 \times LT \times PBT) \quad (4)$$

Table 4.1 ANOVA Table for Tensile Strength Model

Source	DF	SS	MS	F	P	R^2	Remarks
Regression	9	266.541	29.6157	92.29	0	0.981	$F_{0.01,9,10}$ = 4.94; F > $F_{0.01,9,10}$; model is adequate
Linear	3	151.700	9.839	30.66	0		
Square	3	0.341	0.1136	0.35	0.787		
Interactions	3	114.500	38.1667	118.93	0		
Residual Error	10	3.209	0.3209				$F_{0.01,5,10}$=5.64; F < $F_{0.01,5,10}$; lack of fit is insignificant
Lack of fit	5	1.876	0.3752	1.41	0.359		
Pure Error	5	1.333	0.2667				
Total	19	269.750					

It is required to check the model fitness in order to analyze the acquired data. The checking includes the significance of the regression model and the lack of fit. ANOVA is performed to check the models adequacy and is given in table 4.1. The quadratic model is recommended by the fit summary, which realises the tensile strength, is statically adequate with lack of fit found to be insignificant. The value of R^2 is 98.1%, which shows the regression model establishes a very strong correlation between the input parameters and the response (tensile strength). The calculated *F* value of the model is 92.29. In this model, the value of $F_{0.01,9,10}$ is 4.94 for a significance level of $\alpha = 0.01$. This value is less than the *F* value of the model, thereby confirming model accuracy for 99% confidence interval. Further, the *F*-value of lack of fit is 1.41, which is less than $F_{0.01,5,10}$ that is 5.64. This means the lack of fit is insignificant.

Percentage contributions for each term of the model are shown in figure 4.1. It is found that part bed temperature and layer thickness are the most significant parameters

which affects the tensile strength of the parts. The layer thickness is found to be the most significant factor influencing the tensile strength with contribution of 29% which is followed by part bed temperature with contribution of 27%.

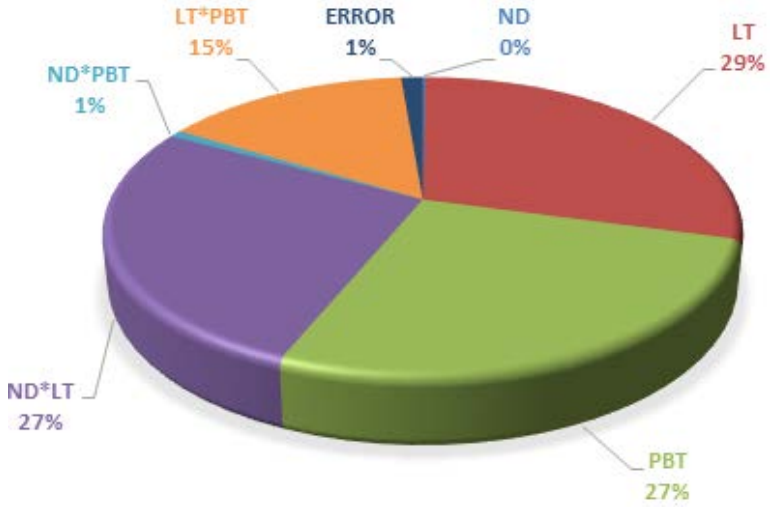

Figure 4.1 Percent contribution of input variables for tensile strength

4.2 RESULT AND DISCUSSION

The main effect plot for tensile strength is shown in figure 4.2. Form the plot it is clear that layer thickness and part bed temperature influences the tensile strength. It can be observed from figure 4.1 & 4.2 that nozzle diameter has negligible effect on tensile strength. Further from figure 4.2 it can be observed that tensile strength of the part increases as the part bed temperature increases and decreases as the layer thickness increases.

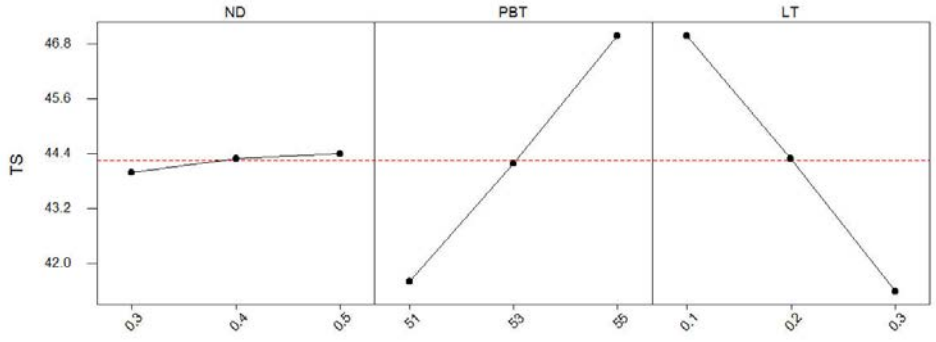

Figure 4.2 Main effect plot for tensile strength

The surface and contour plots for the tensile strength have been drawn using equation (4) with the help of MATLAB software (version 2015a). Surface contour plots provide one of the most revealing ways of illustrating and interpreting the surface design. The variation of tensile strength with respect to part bed temperature can be seen from figure 4.3(a). The surface plot reveals that tensile strength increses with increase in part

bed temperature. As the part bed temperature increases, there is increase in heat dissipation from one layer to another, which leads to post heating of layers which are already bonded. Due to this post heating of layers, greater diffusion of one layer to the adjacent layer occurs and hence improves the strength.

a) b)

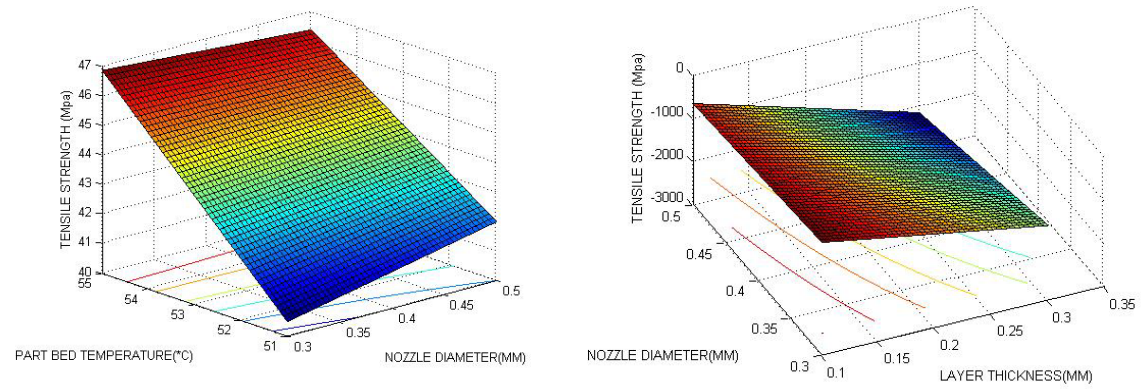

Figure 4.3 Response surfaces for tensile strength

The effect of layer thickness on the value of tensile strength is also presented in figure 4.3(b). It shows that the value of tensile strength increases with decrese of the layer thickness. When layer thickness is high, the amount of heat passing through the layer decreses. As a result, the heat input to the subsequent next layer reduces. However when small layer thickness is considered, the amount of heat available as input to the next layer is higher as compared to the heat input in thick layer. This results in strong inter layer bonding which is an important factor. Further when small layer thickness is considered, more number of layers will be required to build the part. More the number of layers required, higher would be the bonding formed between layers. This results in greater tensile strength at low layer thickness.

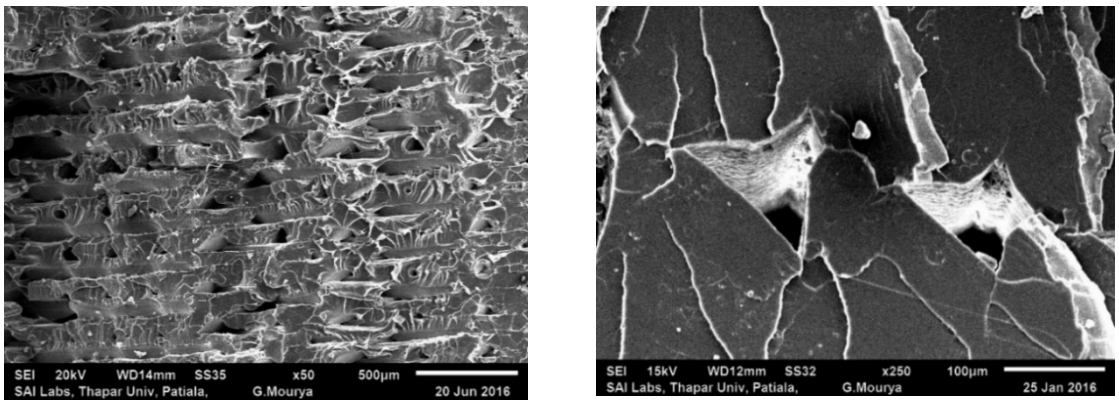

Figure 4.4 SEM micrograph showing voids between layers and rasters

From the SEM micrographs shown in figure 4.4, due to very high scanning speeds, there is formation of voids between the adjacent layers. Layer thickness is one of

the important factor on which the volume of this voids depends. Due to 45^0/-45^0 raster orientation between adjacent layers, when layer thickness is low, large contact area between rasters of same layer and of adjacent layer will occur during bond formation. This will result in strong bond formation. Figure 4.5 shows the SEM image of fractured surface. It can be clearly observed that failure has been caused because of rupturing due to pulling of fibers and rasters.

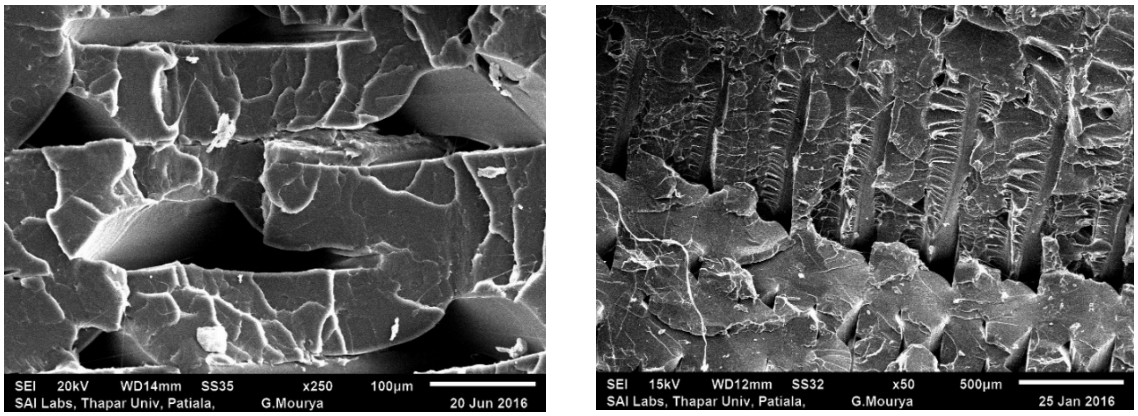

Figure 4.5 SEM image of tensile specimen showing the rupture of fibers

4.3 CONFIRMATION OF EXPERIMENTS

Due to the experimental error, the approximate parameter gives responses, which are subjected to uncertainty. The precision of responses was approximated by computing error in statistical model within confidence interval. The range of predetermined output is $TS \pm \Delta TS$, where ΔTS is calculated by the formula given below:

$$\Delta TS = t_{\alpha/2,DF}\sqrt{(Ve)} \quad (5)$$

Here, ΔTS denotes error in tensile strength, t is the value of t-distribution at the specified degree of freedom (DF), α is the level of confidence interval and Ve is the mean square of residual error in predicted statistical model. The value of α is taken as 0.01. The calculated value of ΔTS is 1.57 Mpa. It can be seen from the confirmation experiments given in table 4.2 & 4.3 that the developed model can predict the tensile strength accurately within 99 % confidence interval.

Table 4.2 Confirmation Experiments (Parameters Selected from the DOE Table)

Exp No.	Machining Parameters			Tensile strength	
	LT (mm)	ND (mm)	PBT (°C)	Experimental (Mpa)	Predicted (Mpa)
1	0.3	0.3	55	50	49.05±1.57
2	0.2	0.4	53	45	43.92±1.57
3	0.1	0.5	55	50	50.15±1.57

4	0.1	0.3	51	43	42.77±1.57

Table 4.3 Confirmation Experiments (Parameters selected from Outside the DOE Table)

Exp No.	Machining Parameters			Tensile strength	
	LT (mm)	ND (mm)	PBT (°C)	Experimental (Mpa)	Predicted (Mpa)
1	0.3	0.2	51	41	40.49±1.57
2	0.4	0.3	51	37	35.96±1.57
3	0.3	0.2	55	46	46.85±1.57
4	0.5	0.1	53	50	50.21±1.57

4.4 OPTIMIZATION OF RESPONSES FOR TENSILE STRENGTH

Tensile strength can be maximized by setting the process parameter at optimum level. The formulation of the problem for maximization will be as follows:

Maximize (TS)

Subjected to $0.1 \leq$ Layer Thickness (mm) ≤ 0.3

$0.3 \leq$ Nozzle Diameter (mm) ≤ 0.5

$51 \leq$ Part Bad Temperature (°C) ≤ 55

Trust region method of non linear maximization is used to find the optimum levels of the parameters. Optimization tool box from the MATLAB 2015a is used for carrying out the optimization. The obtained machine parameter that gives maximum tensile strength is given in Table 4.4.

Table 4.4 Optimum Process Parameter for maximum tensile strength

Exp no	Machining Parameters			Tensile strength (Mpa)	
	LT (mm)	ND (mm)	PBT (°C)	Experimental	Predicted
1	0.1	0.5	51	51	50.15 ± 1.57

4.5 CONCLUSIONS

In the present study, statistical model have been developed to predict tensile strength for 3D Printing process using PLA as work material. For the model, adequacy has been checked by ANOVA and significant parameters have been identified.

The results show that second order models developed for tensile strength is significant. It has been observed that layer thickness and part bed temperature significantly affects the tensile strength. It has been observed that with increase in layer

thickness, tensile strength decresesss. Increase in part bed temperature leads to increase in tensile strength.

Confirmation of the developed model was done by performing experiments at various input variable, which conforms that the prediction of model is precisely within 99% confidence interval. Further, process parameters were optimized to obtain maximum tensile strength for the component.

CHAPTER 5

STATISTICAL MODELING FOR FLEXURAL STRENGTH

5.1 STATISTICAL MODELING

A statistical model for the flexural strength was developed, by correlating the input parameters namely nozzle diameter, layer thickness and part bed temperature based on analysis of the data presented in table 3.6, and is given below as equation (6) after eliminating all the insignificant parameters.

$$FS = -88.7 - (399 \times ND) + (27.0 \times LT) + (7.63 \times PBT) - (292 \times ND \times ND) - (248 \times LT \times LT) - (0.0818 \times PBT \times PBT) - (189 \times ND \times LT) + (3.44 \times ND \times PBT) + (3.69 \times LT \times PBT) \quad (6)$$

It is required to check the model fitness in order to analyze the acquired data. The checking includes the significance of the regression model and the lack of fit. ANOVA is performed to check the models adequacy and is given in table 5.1. The quadratic model is recommended by the fit summary, which realises the flexural strength, is statically adequate with lack of fit found to be insignificant. The value of R^2 is 99.2%, which shows the regression model establishes a very strong correlation between the input parameters and the response (flexural strength). The calculated *F* value of the model is 2000. In this model, the value of $F_{0.01,9,10}$ is 4.94 for a significance level of α = 0.01. This value is less than the *F* value of the model, thereby confirming model accuracy for 99% confidence interval. Further, the *F*-value of lack of fit is 3.63, which is less than $F_{0.01,5,10}$ that is 5.64. This means the lack of fit is insignificant.

Table 5.1 ANOVA Table for flexural strength Model

Source	DF	SS	MS	F	P	R^2	Remarks
Regression	9	382.537	42.5041	2.00E+03	0	0.992	$F_{0.01,9,10}$ = 4.94; $F > F_{0.01,9,10}$; model is adequate
Linear	3	316.289	4.7572	186.77	0		
Square	3	29.615	9.8715	387.57	0		
Interactions	3	36.634	12.2112	479.43	0		
Residual Error	10	0.255	0.0255				$F_{0.01,5,10}$=5.64; $F < F_{0.01,5,10}$; lack of fit is insignificant
Lack of fit	5	0.2	0.0399	3.63	0.092		
Pure Error	5	0.055	0.011				
Total	19	382.792					

Percentage contributions for each term of the model are shown in figure 5.1. The figure shows that layer thickness is the most influential parameters affecting flexural strength with 60% contribution. The contribution of part bed temperature and nozzle diameter, are 12% and 11% respectively.

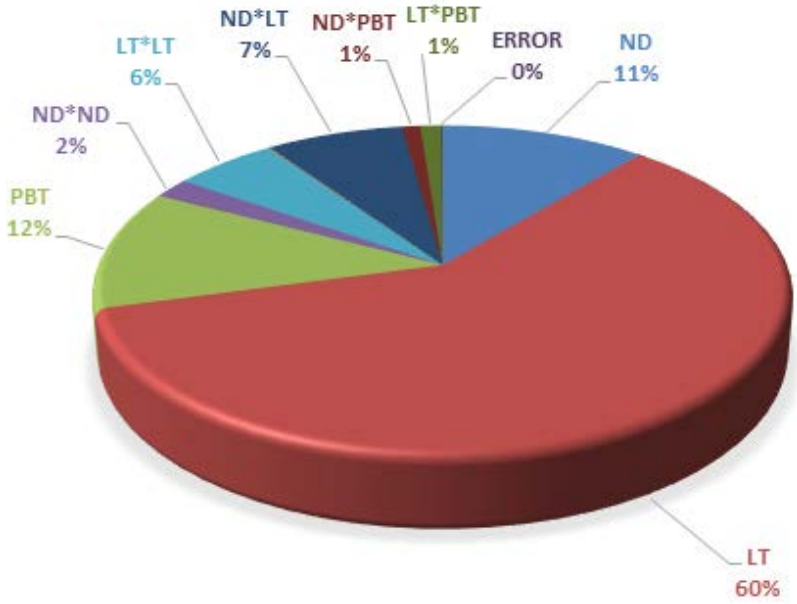

Figure 5.1 Percent contribution of input variables for flexural strength

5.2 RESULT AND DISCUSSION

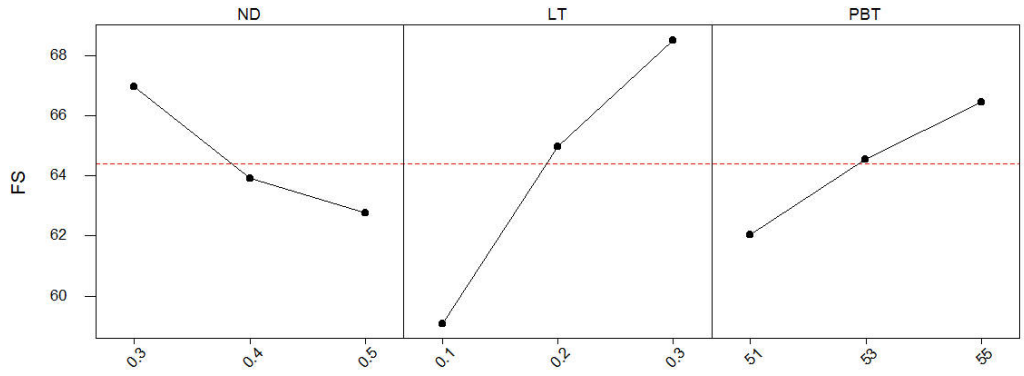

Figure 5.2 Main Effect Plot for flexural strength

The main effect plot for flexural strength is shown in figure 5.2. From the plot, it is evident that all three parameters nozzle diameter, layer thickness and part bed temperature influences the flexural strength. It can be observed from figure 5.1 & 5.2 that layer thickness is most significant parameter. Further from figure 5.2 it can be observed that flexural strength of the part decreses as the nozzle diameter increases. Whereas the flexural strength increases with increase in layer thickness and part bed temperature.

a)

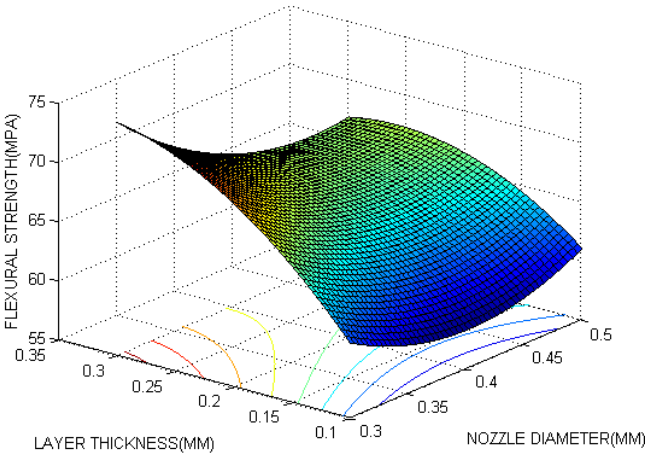

b)

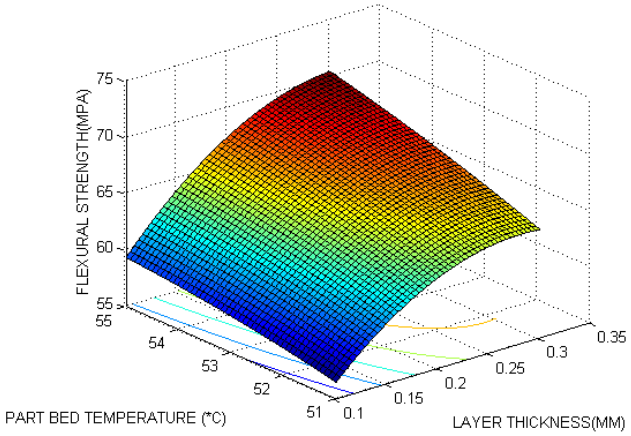

c)

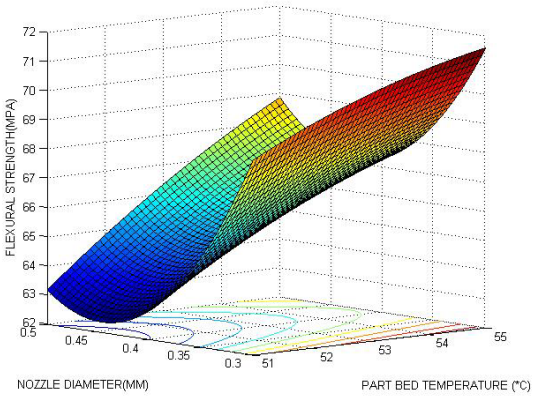

Figure 5.3 Response surfaces for flexural strength

Figure 5.3 shows the surface and contour plots for flexural strength drawn using equation (6) with the help of MATLAB software (version 2015a). The variation of

flexural strength with respect to layer thickness can be seen from figure 5.3 (*a*). In case of flexural testing, the direction of load is normal to the surface of the specimen, which is evident from figure 3.5 (b). So load acting on the rasters is normal loading. In normal loading, thicker rasters are difficult to bend because cross sectional area of rasters is higher as compared to thin rasters, which provides higher rigidity and more strength to the part. This is also evident from figure 5.4 which show the rasters at different layer thicknesses.

a) b)

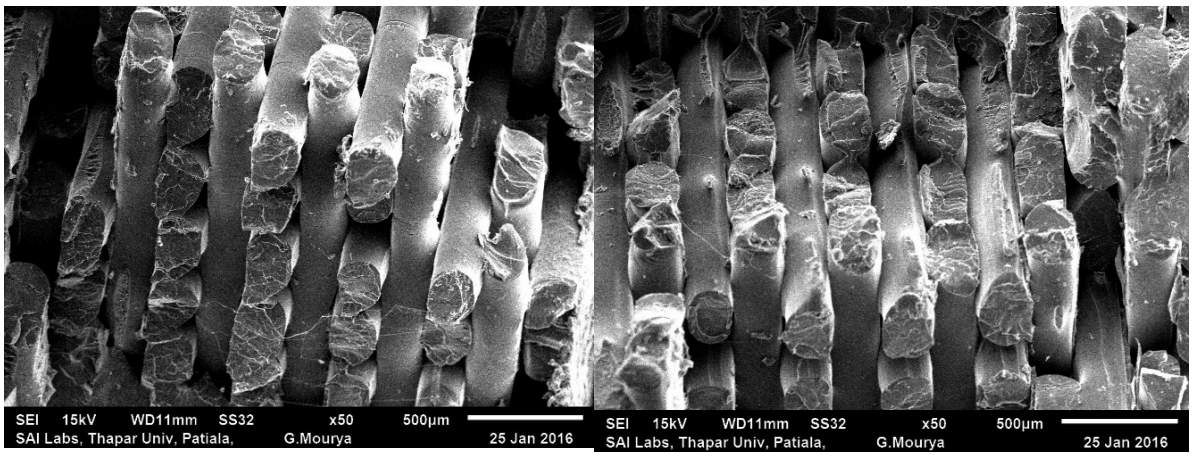

Figure 5.4 SEM image showing raster thickness of a) 100 micrometer b) 300 micrometer

The effect of part bed temperature on the value of flexural strength is presented in figure 5.3 (b). It is observed that an increase in part bed temperature increases the value of strength. As the part bed temperature increases, there is increase in heat dissipation from one layer to another, which leads to post heating of layers which are already bonded. Due to this post heating of layers, greater diffusion of one layer to the adjacent layer occurs and hence improves the strength. It was observed that as the temperature decreases, the deposited fiber acquires a large deformation even with very less force and the capacity to oppose the external force is small, so the strength decreases.

Figure 5.3 (c) shows the effect of nozzle diameter on the flexural strength of the part. It shows that flexural strength decreases with increase in nozzle diameter. It was observed that due to high extruder speed, the material deposited with large nozzle diameter was unable to settle down. The flow of heat was not stable as before the cooling could occur, a new layer was deposited. This resulted in large amount of voids present between the rasters. It was also observed that the size of the void increased as the nozzle diameter was increased as evident in figure 5.5. This presence of voids leads to decrease in flexural strength.

a)

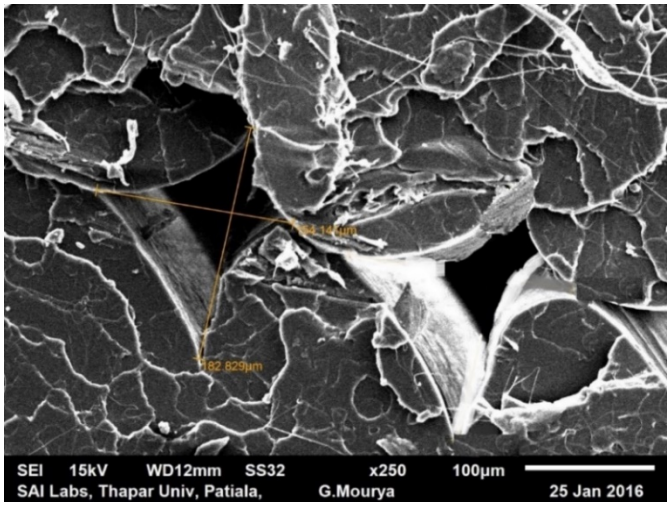

b)

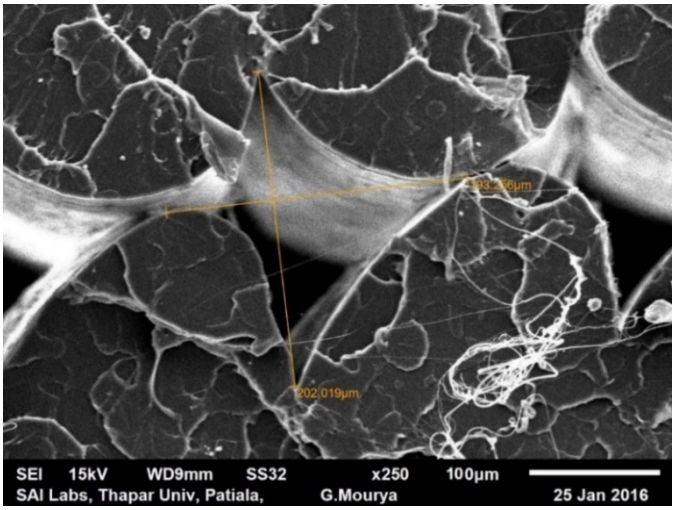

Figure 5.5 SEM image dimensions of voids for nozzle diameter of a) 300 µm b) 500 µm

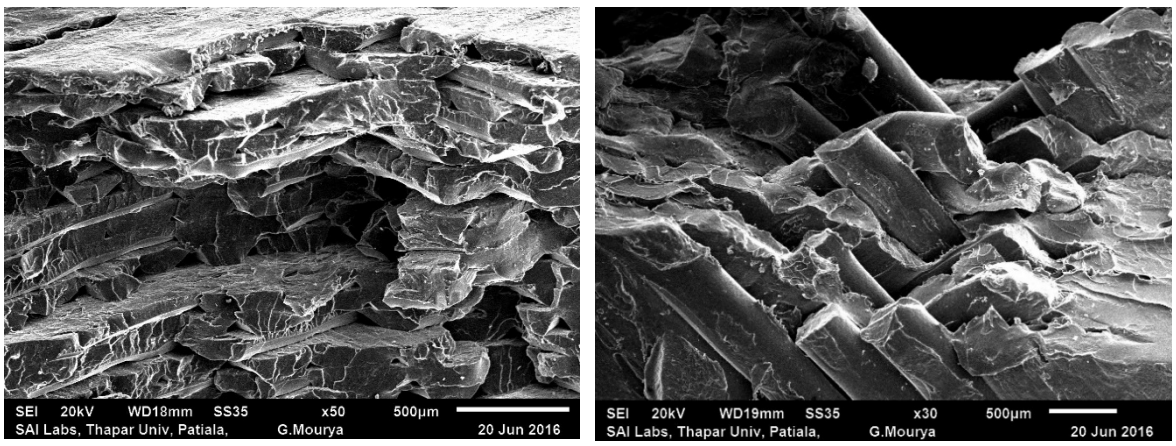

Figure 5.6 SEM image of flexural specimen showing distortion

Fracture behavior of flexural specimen revealed that failure starts at tensile side (bottom side of the part) of the specimen. However the pieces are held together by unbroken fibers of compression side and also crack propagation along load direction is almost straight. Compression side that is the top side of the specimen breaks by bending of the fibers. It was observed from the SEM image given in figure 5.6 that the failure is caused because of bending and fracture of rasters and material.

5.3 CONFIRMATION OF EXPERIMENTS

Due to the experimental error, the approximate parameter gives responses, which are subjected to uncertainty. The precision of responses was approximated by computing error in statistical model within confidence interval. The range of predetermined output is $FS \pm \Delta FS$, where ΔFS is calculated by the formula given below:

$$\Delta FS = t_{\alpha/2,DF}\sqrt{(Ve)} \quad (7)$$

Here, ΔFS denotes error in flexural strength, t is the value of t-distribution at the specified degree of freedom (DF) and Ve is the mean square of residual error in predicted statistical model. The value of α is taken as 0.01. The value of ΔFS is 0.506 Mpa. It can be seen from the confirmation experiments given in Table 5.2 & 5.3 that the developed model can predict the flexural strength accurately within 99 % confidence interval.

Table 5.2 Confirmation Experiments (Parameters Selected from the DOE Table)

Exp No.	Machining Parameters			Flexural strength	
	LT (mm)	ND (mm)	PBT (°C)	Experimental (Mpa)	Predicted (Mpa)
1	0.3	0.3	55	76.2	76.5 ± 0.506
2	0.2	0.4	53	65.2	65.43 ± 0.506
3	0.1	0.5	55	62.5	62.67 ± 0.506
4	0.1	0.3	51	60.1	60.25 ± 0.506

Table 5.3 Confirmation Experiments (Parameters Selected from Outside the DOE Table)

Exp No.	Machining Parameters			Flexural strength	
	LT (mm)	ND (mm)	PBT (°C)	Experimental (Mpa)	Predicted (Mpa)
1	0.3	0.2	51	69.16	68.65 ± 0.506
2	0.4	0.3	51	65.12	64.52 ± 0.506
3	0.3	0.2	55	71.23	71.57 ± 0.506
4	0.5	0.1	53	70.31	60.91± 0.506

5.4 OPTIMIZATION OF RESPONSES FOR FLEXURAL STRENGTH

Flexural strength can be maximized by setting the process parameter at optimum level. The formulation of the problem for maximization will be as follows:

Maximize (FS)

Subjected to $0.1 \leq$ Layer Thickness (mm) ≤ 0.3

$0.3 \leq$ Nozzle Diameter (mm) ≤ 0.5

$51 \leq$ Part Bad Temperature (°C) ≤ 55

Trust region method of non linear maximization is used to find the optimum levels of the parameters. Optimization tool box from the MATLAB 2015a is used for carrying out the optimization. The obtained machine parameter that gives maximum flexural strength is given in Table 5.4.

Table 5.4 Optimum Process Parameter for Maximum flexural strength

Exp no	Machining Parameters			Flexural strength (Mpa)	
	LT (mm)	ND (mm)	PBT (°C)	Experimental	Predicted
1	0.3	0.3	55	76.2	76.5 ± 0.506

5.5 CONCLUSIONS

In the present study, statistical models have been developed for predicting flexural strength for 3D Printing process using PLA as work material. For the models, adequacy has been checked by ANOVA and significant parameters have been identified.

The results show that second order models developed for flexural strength is significant. It has been observed that layer thickness is the most significant parameter that affects the flexural strength. It has been observed that with increase in layer thickness and part bed temperature, flexural strength increases, but increase in nozzle diameter will reduce the flexural strength.

Confirmation of the developed model was done by performing experiments at various input variable, which conforms that the prediction of model is precisely within 99% confidence interval. Further, process parameters were optimized to obtain maximum flexural strength for the component.

CHAPTER 6

STATISTICAL MODELING FOR IMPACT STRENGTH

6.1 STATISTICAL MODELING

A statistical model for the impact strength was developed, by correlating the input parameters namely nozzle diameter, layer thickness and part bed temperature based on analysis of the data presented in table 3.6, and is given below as equation (8) after eliminating all the insignificant parameters.

$$IS = 166 - (11.9 \times ND) + (9.98 \times LT) - (6.12 \times PBT) + (11.9 \times ND \times ND) - (10.1 \times LT \times LT) + (0.0579 \times PBT \times PBT) + (6.81 \times ND \times LT) + (0.0294 \times ND \times PBT) - (0.147 \times LT \times PBT) \quad (8)$$

It is required to check the model fitness in order to analyze the acquired data. The checking includes the significance of the regression model and the lack of fit. ANOVA is performed to check the models adequacy and is given in table 6.1. The quadratic model is recommended by the fit summary, which realises the impact strength, is statically adequate with lack of fit found to be insignificant. The value of R^2 is 99.7%, which shows the regression model establishes a very strong correlation between the input parameters and the response (impact strength). The calculated *F* value of the model is 2000. In this model, the value of $F_{0.01,9,10}$ is 4.94 for a significance level of $\alpha = 0.01$. This value is less than the *F* value of the model, thereby confirming model accuracy for 99% confidence interval. Further, the *F*-value of lack of fit is 1.88, which is less than $F_{0.01,5,10}$ that is 5.64. This means the lack of fit is insignificant.

Table 6.1 ANOVA Table for Impact Strength

Source	DF	SS	MS	F	P	R^2	Remarks
Regression	9	0.495497	0.055055	2000.00	0	0.997	$F_{0.01,9,10}$ = 4.94; F > $F_{0.01,9,10}$; model is adequate
Linear	3	0.109017	0.05929	2000.00	0		
Square	3	0.342172	0.114057	4000.00	0		
Interactions	3	0.044307	0.014769	461.32	0		
Residual Error	10	0.00032	0.000032				$F_{0.01,5,10}$=5.64; F < $F_{0.01,5,10}$; lack of fit is insignificant
Lack of fit	5	0.000209	0.000042	1.88	0.253		
Pure Error	5	0.000111					
Total	19	0.495817	0.000022				

Percentage contributions for each term of the model are shown in figure 6.1. The figure shows that layer thickness is the most influential parameters affecting impact

strength. The layer thickness is found to be the most significant factor with contribution of 16% followed by nozzle diameter which is 6 %. Part bed temperature has negligible effect on impact strength.

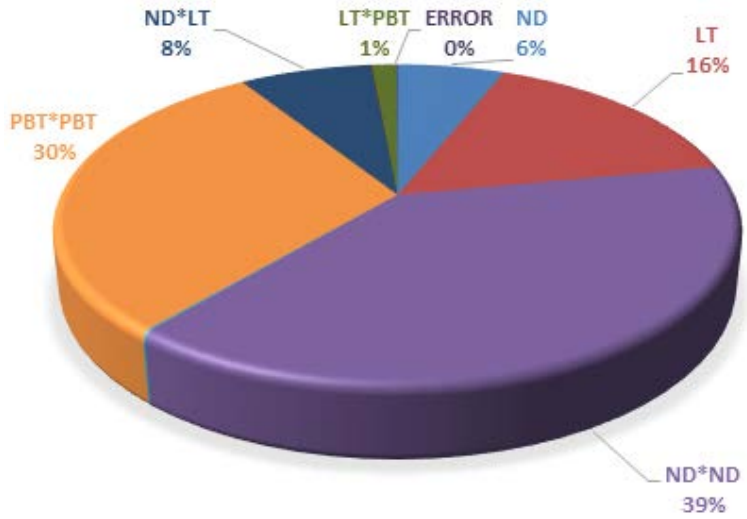

Figure 6.1 Percent contribution of input variables for impact strength

6.2 RESULT AND DISCUSSION

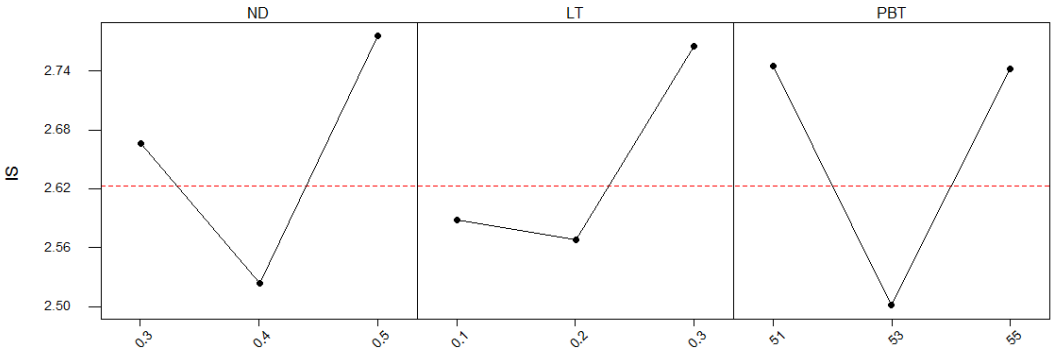

Figure 6.2 Main Effect Plot for Impact strength

The surface and contour plots for the impact strength drawn using equation (8) with the help of MATLAB software (version 2015a). Surface contour plots provide one of the most revealing ways of illustrating and interpreting the surface design. From the main effect plot, it is evident that nozzle diameter and layer thickness influences the impact strength. It can be observed from figure 6.1 & 6.2 that layer thickness is most significant parameter. Further from figure 6.2, it can be observed that impact strength of the part fluctuates as the nozzle diameter and layer thickness increases.

The variation of impact strength with respect to layer thickness can be seen from figure 6.3. It is observed that impact strength increses with increase in layer thickness. As the layer thickness increases, the diameter of the rasters also increase, thereby providing

higher rigidity and more strength to the part. Thicker rasters are difficult to bend, as a result they have more shock load bearing capacity thereby improving the impact strength.

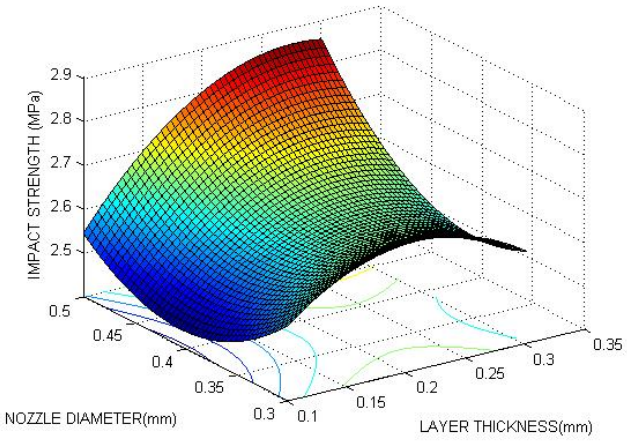

Figure 6.3 Response surfaces for Impact strength

The effect of nozzle diameter on the value of impact strength is also presented in figure 6.3. It is observed that, on increase of nozzle diameter, impact strength initially decreased and then after a certain value of nozzle diameter, it increased. It was observed that at a temperature range near the glass transition temperature, the deposited fiber acquires a large deformation even with very less force. Further, the capacity to resist the outside force is small. As a result, the impact strength is reduced. However, in spite of shrinkage and contraction, the inner stresses are not accumulated. As the temperature and nozzle diameter increases, the heat conduction towards bottom layers results in increase in the temperature at bonding interface and hence, proper diffusion takes place between adjacent rasters. Therefore, the bonding strength increases which is reflected in the increase in impact strength. Also increase in nozzle diameter results in greater deposition of material, which also increases the impact strength. SEM image of fracture surface for impact specimen is shown in figure 6.4 indicates failure by sudden rupture of rasters.

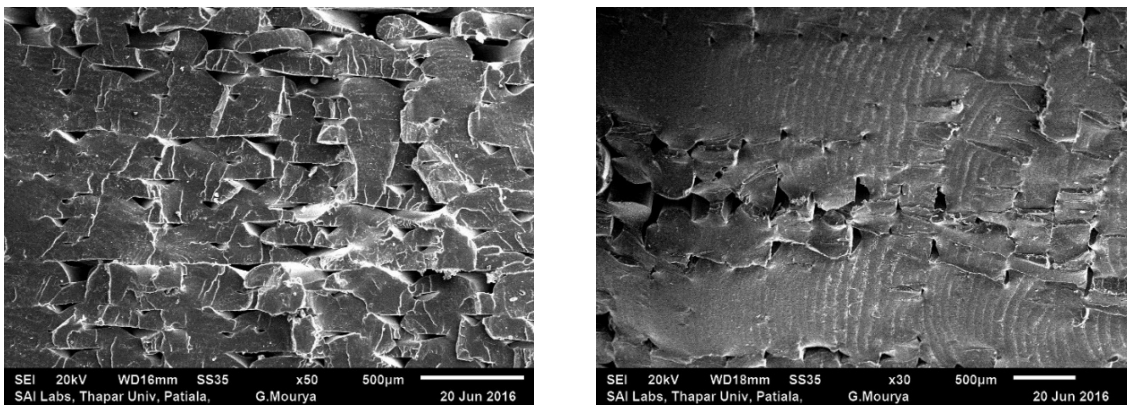

Figure 6.4 Fracture surface of impact specimen

6.3 CONFIRMATION OF EXPERIMENTS

Due to the experimental error, the approximate parameter gives responses, which are subjected to uncertainty. The precision of responses was approximated by computing error in statistical model within confidence interval. The range of predetermined output is $IS \pm \Delta IS$, where ΔIS is calculated by the formula given below:

$$\Delta IS = t_{\alpha/2,DF}\sqrt{(Ve)} \quad (9)$$

Here, ΔIS denotes the error in impact strength, t is the value of t-distribution at the specified degree of freedom (DF) and Ve is the mean square of residual error in predicted statistical model. The value of α is taken as 0.01. The value of ΔIS is 0.016 KJ/m^2. It can be seen from the confirmation experiments given in Table 5.2 & 5.3 that the developed model can predict the tensile strength accurately within 99 % confidence interval.

Table 6.2 Confirmation Experiments (Parameters Selected from the DOE Table)

Exp No.	Machining Parameters			Impact strength	
	LT (mm)	ND (mm)	PBT (°C)	Experimental (KJ/m^2)	Predicted (KJ/m^2)
1	0.3	0.3	55	2.677	2.676 ± 0.016
2	0.2	0.4	53	2.496	2.498 ± 0.016
3	0.1	0.5	55	2.676	2.679 ± 0.016
4	0.1	0.3	51	2.648	2.649 ± 0.016

Table 6.3 Confirmation Experiments (Parameters Selected from Outside the DOE Table)

Exp No.	Machining Parameters			Impact strength	
	LT (mm)	ND (mm)	PBT (°C)	Experimental (KJ/m^2)	Predicted (KJ/m^2)
1	0.3	0.2	51	2.806	2.801 ± 0.016
2	0.4	0.3	51	2.745	2.748 ± 0.016
3	0.3	0.2	55	2.781	2.785 ± 0.016
4	0.5	0.1	53	2.419	2.413 ± 0.016

6.4 OPTIMIZATION OF RESPONSES FOR IMPACT STRENGTH

Impact strength can be maximized by setting the process parameter at optimum level. The formulation of the problem for maxmization will be as follows:

Maximize (IS)

Subjected to $0.1 \leq$ Layer Thickness (mm) ≤ 0.3

$0.3 \leq$ Nozzle Diameter (mm) ≤ 0.5

$51 \leq$ Part Bad Temperature (°C) ≤ 55

Trust region method of non linear maximization is used to find the optimum levels of the parameters. Optimization tool box from the MATLAB 2015a is used for carrying out the optimization. The obtained machine parameter that gives maximum impact strength is given in Table 6.4.

Table 6.4 Optimum Process Parameter for Maximum Impact strength

Exp no	Machining Parameters			Impact strength (KJ/m^2)	
	LT (mm)	ND (mm)	PBT (°C)	Experimental	Predicted
1	0.3	0.3	55	2.958	2.947 ± 0.016

6.5 CONCLUSIONS

In the present study, statistical models have been developed for predicting impact strength for 3D Printing process using PLA as work material. For the models, adequacy has been checked by ANOVA and significant parameters have been identified.

The results show that second order models developed for impact strength is significant. It has been observed that layer thickness is the significant parameter that affects the impact strength as compared to the nozzle diameter and part bed temperature. As the layer thickness increases, impact strength increases. It is also observed that, on increase of nozzle diameter, impact strength initially decreased and then after a certain value of nozzle diameter, it increased.

Confirmation of the developed model was done by performing experiments at various input variable, which conforms that the prediction of model is precisely within 99% confidence interval. Further, process parameters were optimized to obtain maximum impact strength for the component.

CHAPTER 7
CONCLUSION AND SCOPE FOR THE FUTURE WORK

7.1 SUMMARY OF THE PRESENT RESEARCH

In the present study, investigations into the tensile strength, flexural strength and impact strength have been performed for solidified PolyLactic Acid (PLA) parts fabricated using 3D Printing process. Statistical models have been developed for predicting tensile strength, flexural strength and impact strength by correlating the input parameters, namely, layer thickness, nozzle diameter and part bed temperature. Specimens were fabricated and tested for the study. For all the developed strength models, significant parameters have been identified and ANOVA has been used to establish the adequacy of the models.

The results show that second order model developed for tensile strength is statistically significant. It has been observed that layer thickness and part bed temperature significantly affects the tensile strength. It has been observed that with increase in layer thickness, tensile strength decresesss, whereas increase in part bed temperature leads to increase in tensile strength.

The second order model developed for flexural strength has been found to be statistically significant. It has been observed that layer thickness is the most significant parameter that affects the flexural strength followed by part bed temperature and nozzle diameter. Results showed that increase in layer thickness and part bed temperature, increased the flexural strength however increase in nozzle diameter reduces the flexural strength.

Further it was observed that second order models developed for impact strength is also statistically significant. It has been observed that layer thickness is the significant parameter that affects the impact strength followed by nozzle diameter. It has been observed that as the layer thickness increases, impact strength increases. It was observed that, on increase of nozzle diameter, impact strength initially decreased and then after a certain value of part bed temperature, it increased.

Confirmation experiments were conducted at various test conditions to show that the developed models can predict tensile strength, flexural strength and impact strength values accurately within 99% confidence interval. Further optimal process parameters have been identified for obtaining maximum tensile strength, flexural strength and impact strength.

7.2 MAJOR CONCLUSIONS OF THE PRESENT WORK

Based on the work presented in previous chapters and summary presented above, the following conclusions are drawn from the present research work.

- Statistical models have been developed for predicting tensile strength, flexural strength and impact strength of part.
- Confirmation experiments were conducted at various test conditions, which showed that the developed models for tensile strength, flexural strength and impact strength could predict strength values accurately within 99% confidence interval.
- Optimal process parameters have been identified for obtaining maximum tensile strength, flexural strength and impact strength.
- The results show that second order models developed for tensile strength, flexural strength and impact strength are statistically significant.
- It has been observed that layer thickness and part bed temperature significantly affects the tensile strength.
- For flexural strength, it has been observed that layer thickness is the most significant parameter followed by part bed temperature and nozzle diameter.
- It has been observed that layer thickness is the significant parameter that affects the impact strength followed by nozzle diameter.

7.3 SCOPE FOR FUTURE WORK

- Effect of orientation can be studied on part strength.
- Genetic algorithm can be applied for optimization of the part strength.
- This work can be further extended on to other materials like Nylon, HIPS, Polycarbonate etc..

REFERENCES

1. Chua, C.K.; Leong, K.F.; Lim, C.S. (2000) Rapid Prototyping: Principles and Applications in Manufacturing, John Wiley and Sons Inc.
2. Pandey, P. M. (2010) Rapid Prototyping Technologies, Applications and Part Deposition Planning, IIT Delhi.
3. Williams, J. D.; Deckard, C. R.; (1998) Advances in modeling the effects of selected parameters on the SLS process. *Rapid Prototyping Journal* 4, no. 2: 90-100.
4. Ahn, S. H.; Montero, M.; Odell, D.; Roundy, S.; Wright, P. K. (2002) Anisotropic material properties of fused deposition modeling ABS. *Rapid Prototyping Journal*, no. 4: 248–257.
5. Ang, K. C.; Leong, K. F.; Chua, C. K. (2006) Investigation of the mechanical properties and porosity relationships in fused deposition modelling-fabricated porous structures. *Rapid Prototyping Journal*, no. 12(2): 100-105.
6. Jain, P. K.; Pandey, P. M.; Rao, P. V. M. (2009) Effect of delay time on part strength in selective laser sintering. *International Journal Of Advanced Manufacturing Technology*, no. 43: 117-126.
7. Bagsik, A.; Schoeppner, V.; Klemp, E. (2010) FDM Part Quality Manufactured with Ultem*9085. In proceedings of 14th International Scientific Conference on Polymeric Materials.
8. Kesy, A.; Kotlinski, J. (2010) Mechanical properties of parts produced by using polymer jetting technology. Technical University of Radom, Malczewskiego 29, 26-600 Radom, Poland. Vol. X,2010.
9. Percoco, G.; Lavecchia F.; Galantucci, L. M. (2012) Compressive Properties of FDM Rapid Prototypes Treated with a Low Cost Chemical Finishing. *Research Journal of Applied Sciences, Engineering and Technology*, no. 4 (19): 3838-3842.
10. Croccolo, D.; Agostinis, M. D.; Olmi, G. (2013) Experimental characterization and analytical modelling of the mechanical behavior of fused deposition processed parts made of ABS-M30.*Computational Materials Science*, no. 79: 506-518
11. Afrose, F.; Masood, S. H.; Iovenitti, P.; Nikzad, M.; Sbarski, I. (2015) Effects of part build orientations on fatigue behavior of FDM processed PLA material. *Progress in Additive Manufacturing*, DOI 10.1007/s40964-015-0002-3.

12. Roberson, D. A.; Perez, A. R. T.; Shemelya, C. M.; Rivera, A.; MacDonald, E.; Wicker, R. B. (2015) Comparison of stress concentrator fabrication for 3D printed polymeric izod impact test specimens. *Additive Manufacturing*, no. 7: 1-11.
13. Montgomery, D. C. (2008) *Design and analysis of experiments*. John Wiley & Sons.
14. ASTM (2010) D638-10. Standard test method for tensile properties of plastics. American Society for Testing and Materials, USA
15. ASTM (2010) D790-10. Standard test method for flexural properties of plastics. American Society for Testing and Materials, USA
16. ISO (2010) 180. Standard test method for impact properties of plastics. International Organization for Standardization, Switzerland.

WEB REFERENCES

A. http://nptel.ac.in/courses/112102103//Module%20G/Module%20G(4)/p2.htm (Accessed on – 12/04/2015).
B. http://www.custompartnet.com/wu/stereolithography. (Accessed on – 20/04/2015).
C. http://www.azom.com/article.aspx?ArticleID=1650 (Accessed on – 20/04/2015).
D. https://fused-deposition.wikispaces.com/Fused+Deposition (Accessed on – 03/08/2015).
E. http://3dprinting.com/what-is-3d-printing (Accessed on – 23/08/2015).
F. http://www.rpmandassociates.com/RPMILaserDepositionTechnologyAdvancesAdditiveManufacturingAndRepair.aspx (Accessed on – 09/09/2015).
G. http://www.amse.org.cn/article/2015/1006-7191-28-7-892.html (Accessed on – 17/11/2015).
H. http://www.titaninnovativedesigns.ca/pdf/PLA.pdf (Accessed on – 05/04/2016).

LIST OF PUBLICATIONS

1. Jagdish Khatwani, Vineet Srivastava, “Effect of process parameters on mechanical properties of solidified PLA parts fabricated by 3D Printing process”, accepted in 6th International Conference on 3D Printing & Additive Manufacturing Technologies (AMSI 2016), Bangalore, INDIA, October 6-7 (2016).

pelg.docx

ORIGINALITY REPORT

19%	7%	17%	%
SIMILARITY INDEX	INTERNET SOURCES	PUBLICATIONS	STUDENT PAPERS

PRIMARY SOURCES

1	ethesis.nitrkl.ac.in Internet Source	2%
2	Srivastava, V., and P. M. Pandey. "Experimental investigation on electrical discharge machining process with ultrasonic-assisted cryogenically cooled electrode", Proceedings of the Institution of Mechanical Engineers Part B Journal of Engineering Manufacture, 2013. Publication	2%
3	Sood, A.K.. "Parametric appraisal of mechanical property of fused deposition modelling processed parts", Materials and Design, 201001 Publication	1%
4	Prashant Jain. "Experimental investigations for improving part strength in selective laser sintering", Virtual and Physical Prototyping, 09/2008 Publication	1%